

Exchanges

No 45 (Volume 13, No. 2)

April 2008

North American Monsoon Experiment: NAME

From Munoz-Arriola et al., page 24 : *Extended West-wide Seasonal Hydrological System: Seasonal Hydrological Prediction in the NAMS region*

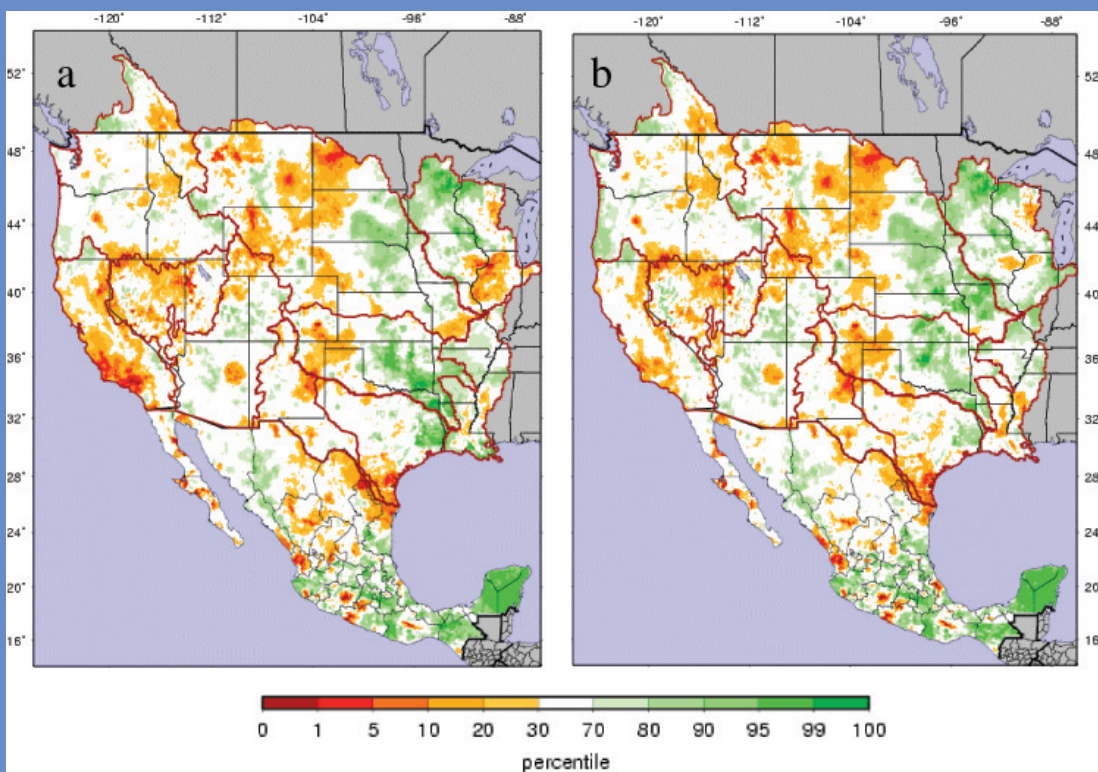


Figure 1: Soil Moisture Percentiles with respect to the 1960-1999 climatology for a) January 1st 2008 and b) January 15th 2008

CLIVAR is an international research programme dealing with climate variability and predictability on time-scales from months to centuries. **CLIVAR** is a component of the World Climate Research Programme (WCRP). WCRP is sponsored by the World Meteorological Organization, the International Council for Science and the Intergovernmental Oceanographic Commission of UNESCO.



Farewell to a scientist and a friend



CLIVAR, NOCS and the science community lost a valued colleague and friend when Peter Killworth died on 28 January after a long battle with Motor Neurone Disease. Peter was co-Chair of the Scientific Steering Group of WCRP's World Ocean Circulation Experiment (WOCE) from 1999 - 2002.

Peter will be remembered for his unbridled enthusiasm for science, his dedication to work, and his selfless and generous nature that fostered and encouraged the scientific development of the numerous colleagues he worked with. Many of the PhD students and postdoctoral workers that he supervised are now leading figures in oceanography in their own right, having received an unparalleled start to their research careers from Peter.

With interests across the whole of physical oceanography (including ice, polynyas, Rossby waves, instabilities and eddies), as well as making a world-class contribution to the study of social networks, Peter's phenomenal published output exceeded 160 scientific papers. He was recently awarded the Stommel Research Medal by the American Meteorological Society for "his many important contributions to ocean modelling and theoretical oceanography", a sentiment echoed by his colleagues and friends around the world.

Peter obtained his PhD on analytical and numerical models of ocean circulation in 1972 from the University of Cambridge. After a postdoctoral position at Scripps Institution of Oceanography in the US, he returned to work in Cambridge with his PhD supervisor, Adrian Gill. In 1985 he joined NERC when moving to the Robert Hooke Institute (RHI) in Oxford, where he built and led a research team at the forefront of numerical ocean modelling. After closure of the RHI, he moved to Southampton to continue his work, building another successful research

team, focused on process modelling. Whilst here, he became the founding editor of the journal, *Ocean Modelling*, of which he was rightly proud. This has rapidly become established as one of the leading journals in the field of oceanography.

Peter will be sorely missed by the many people who knew him and worked with him. His outstanding contribution to oceanography will live on through his published papers, and in the hearts and minds of those who knew him. He is survived by his wife, Sarah, and two sons, Paul and Andrew.

Editorial

As well as its focus on CLIVAR's Variability of the American Monsoon System (VAMOS) North American Monsoon Experiment, NAME, this edition of *Exchanges* also outlines initiatives on dust cycle research and a new programme (PACSWIN) being developed to further study the region of the Indonesian Seas. In addition, a paper by SCOR/IAPSO Working Group 127 seeks input from the community related to improved seawater dynamics on how to implement a proposed change in reporting of salinity. If you have an interest in the salinity issue, please submit your views to Trevor McDougal at the contact email address given in the last paragraph of the article.

By the time this edition of *Exchanges* is finalized, we will have had the 29th annual meeting of the Joint Scientific Committee (JSC) for WCRP and which the CLIVAR SSG co-chairs and I will be attending. As well as reviewing progress and providing direction on a wide variety of issues, the JSC will be considering the future shape of WCRP following the sunset of CLIVAR and its sister projects over the first five years of the next decade. These will be important discussions and we hope to provide an article on the outcomes of the JSC in the next edition of *Exchanges*, due out in July.

Howard Cattle

A view from the golden years of the North American Monsoon Experiment

Gochis, D.J.,
Chair, NAME Science Working Group; National Center for Atmospheric Research
Corresponding author: gochis@rap.ucar.edu

The North American Monsoon Experiment (NAME) is a ten year, international, multi-agency and multi-institution research program aimed at improving predictions of warm season precipitation over North America associated with variations in the North American Monsoon (NAM) system. Full details on NAME programmatic activities and access to all NAME datasets is available online at: <http://www.eol.ucar.edu/projects/name/>. [An outline of the multi-scale NAME research domain covering southwestern North America is provided in Figure 1 of Gutzler et al., page 6] Under the endorsement of the international CLIVAR and GEWEX programs and through funding support of NOAA, NASA, and NSF in the U.S. and the Consejo Nacional de Ciencia y Tecnologia (CONACyT) and Servicio Meteorologico Nacional (SMN) of Mexico, the NAME research program has identified and answered many key scientific questions underpinning the structure and seasonal evolution of the NAM regional climate, its spatial and temporal modes of variability, and key hydroclimatic processes. Beginning in late 2000, a science and implementation plan (NAME Science Working Group, 2008) was developed which identified key process-based questions aimed at addressing

fundamental uncertainties in the function of the monsoon system that were known to be limiting predictive capabilities at that time (see also Higgins et al., 2003). Planning and organization of NAME activities culminated in the design and execution of an intensive continental scale field campaign, or Enhanced Observing Period (EOP), over northwest Mexico and the southwestern U.S. during the boreal summer of 2004 (Higgins et al., 2006). The 2004 EOP provided an unprecedented opportunity to collect detailed information on the exchange and transport of energy and water within the NAM system while also providing a unique opportunity to ingest and evaluate the impact of special observations on operational monitoring and prediction products. Equally important, planning and execution of the 2004 NAME EOP also served to significantly enhance international collaboration between U.S. and Mexican universities and operational weather, climate and water agencies. A first generation of scientific findings from the 2004 NAME EOP has been synthesized in a special issue of the *Journal of Climate* (vol. 20, No. 7), which contained more than 20 articles on diagnostic and modeling studies of the NAM.

This special issue of CLIVAR *Exchanges* brings together a

'second' generation of NAME research since the 2004 EOP and discusses what challenges and opportunities lie ahead in the remaining few years of the NAME program. The short articles that follow present summaries of recent diagnostic and prediction studies that continue to extend our understanding of the behavior of the NAM system and as well as important assessments of our observational and modeling systems. The article by Gutzler et al. summarizes findings from the second phase of the North American Monsoon Assessment Project (NAMAP-see Gutzler et al., 2005 for details from Phase I of NAMAP) and highlights key advances and lingering issues related to seasonal simulation of the NAM system. Next Higgins et al. and Mejia and Douglas evaluate the role of tropical disturbances (e.g. tropical cyclones and tropical easterly waves) on precipitation variability in the monsoon region, specifically, and the U.S. and Mexico, in general. Rowe et al. and Kursinski et al., then present findings on the structure of rainfall and water vapor, respectively, using emerging instrument platforms that were deployed during the 2004 NAME EOP. Vivoni et al. present results from ongoing field work aimed at characterizing the nature of land-atmosphere coupling using field observations and, lastly, Munoz et al. outline the development of a seasonal hydrologic forecast system for the western U.S. and Mexico. The 2007 Journal of Climate special issue, the studies presented here, as well as others that continue to emerge in the literature, represent a significant scientific return on the investment that has been made into improving process understanding and predictions of warm season precipitation over North America. However, the combined advances in NAME research also leave us with several remaining issues (both scientific and programmatic) important to fully realizing the potential predictability that exists within the NAM system.

The remaining paragraphs of this overview piece are aimed at identifying critical gaps in our understanding of hydroclimatic processes within the NAM, defining a few emerging advances in predictive capabilities and summarizing a subset of community activities aimed at synthesizing and transferring NAME research findings to the broader scientific and societal applications communities. Particular emphasis is placed on the critical role of sustained multi-scale observations in advancing diagnostic and prediction research. The discussion of these issues is broken out into three topical areas; NAM Precipitation Processes, Modeling and Prediction Studies, Program Synthesis and Remaining Challenges. While it is impossible to integrate all of the recent and ongoing work related to NAM research, the articles in this special issue and those challenges and opportunities discussed below represent an important snapshot of advances in NAME research as we begin to look forward to transitioning NAME into other programmatic goals aimed at improving predictions of the climate system. Investigators in the CLIVAR community and beyond who are conducting diagnostic and prediction research relevant to the NAM system are strongly encouraged to contact the NAME Science Working Group so that their progress can be integrated into the broader research and prediction goals of NAME.

Precipitation processes in the North American Monsoon

One of the leading accomplishments of the NAME research program has been a much improved characterization of the spatial and temporal patterns of warm season precipitation across the NAM region. Summarized in several recent articles (e.g. Gebremicheal et al., 2007; Gochis et al., 2004 and 2007b; Hong et al., 2007; Janowiak et al., 2007; Lang et al., 2007; Nesbitt et al., 2008; and Rowe et al; 2008) the diurnal cycle and regional variability of clouds and rainfall as it relates to complex terrain and continental-maritime regimes is now much

clearer. This pattern is described as one where precipitation initiates shortly after midday, and most frequently, over the high elevations of the western slope of the Sierra Madre Occidental (SMO) mountains, but with a modest intensity, and later in the afternoon and evening but less frequently and often with greater intensity at lower elevations. Precipitation is also much less frequent, generally occurs at night or in the early morning hours and is generated from significantly shallower clouds over the waters of the Gulf of California than over land. Latitudinally, precipitation varies with decreasing frequency (in terms of daily precipitation) from the south (~22 deg N) northward into the southwestern U.S. Regional variations of rainfall are strongly linked to synoptic-scale disturbances, particularly along the northern and eastern peripheries of the monsoon region in northwest Mexico and southwest U.S.

A conceptual model of the diurnally-evolving structure of clouds and precipitation has recently been put forth in Nesbitt et al. (2008) and is shown in Figure 1. However, this model lacks significant details, particularly with regards to microphysical processes and the structure of diurnally-forced terrain circulations (c.f. Ciesielski and Johnson, 2008), which are critical to developing reliable remotely-sensed quantitative precipitation estimates (QPEs) and to improve model-based quantitative precipitation forecasts (QPFs). For instance, current space-borne remotely-sensed platforms can possess differences greater than 60% in mean daily rainfall estimates over the monsoon region of western Mexico when compared with composites of surface gauge observations (Gochis et al., 2008). However, it is clear that tangible benefit, in terms of QPE error characteristics, can be derived through real-time gauge correction procedures, even if the number of gauges used is relatively small. To continue progress in QPEs over the NAM region, data impact studies are needed to a) identify key informational sources on rainfall characteristics using surface gauge networks such as those described by Lobato et al. (2007), Gochis et al. (2004) and Vivoni et al. (2007), and b) to better integrate observational and modeling research into the characterization of cloud microphysical processes over the NAM region with the goal improving remotely-sensed precipitation retrieval algorithms. In turn, these studies in NAM precipitation processes need to be linked to larger efforts aimed at improving QPE and QPF efforts ongoing within NOAA, NASA, in the U.S. and the SMN and the Comision Nacional del Agua (CONAGUA) of Mexico.

Modeling and prediction studies

Work conducted under the NAMAP effort represents a key achievement in simulation and prediction research under

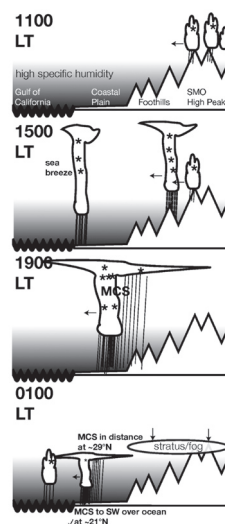


Figure 1: Schematic of observed diurnal mechanisms along the SMO at 25°N. Cloud type indicates relative height attained by clouds, shading indicates specific (not relative) humidity contrasts, asterisks (*) indicate mixed-phase microphysical processes, and density of vertical streaks indicate the location and relative intensity of precipitation. From Nesbitt et al., 2008.

NAME. Phase I results from NAMAP highlighted significant differences between regional and global models in the ability to simulate regional variations in the monsoon, particularly monsoon onset and demise, as well as the diurnal cycle of rainfall and land surface fluxes (Gutzler et al., 2005). Beyond model performance evaluation, though, work conducted under NAMAP has provided the community with a suite of model evaluation metrics (see article by Gutzler et al. below) important for assessing monsoon variability in models and in observational data sets. Metrics similar to these are now being used in the newly developed NAME Forecast Forum which aims to synthesize and intercompare a suite of seasonal prediction models being run at operational modeling centers in the U.S. and Mexico (contact author for details). Moreover, work conducted under NAMAP has exposed critical deficiencies in our operational observing systems which are used to evaluate models. These early findings, in part, provided the motivation for the quantitative assessment work described in the previous sections.

An example of the sensitivity in the interplay between models and observations is provided in Figure 2, page 15 (from Gochis et al., 2008). Here we have driven an operational version of the Noah land surface model (Ek et al., 2003) with identical meteorological forcing except for the specification of different remotely-sensed QPE products. It is clearly evident that land surface hydrological fluxes of surface evapotranspiration (ET), accumulated runoff (Q) and the total runoff fraction (Qr) vary substantially between simulations. Although the coarsest scale (e.g. O1000 km) spatial distribution of simulated ET and runoff are similar between model runs, there are marked differences, in excess of 100% of the range in values given, in the magnitude and regional scale (e.g. O100's km) variability of fluxes. These differences are on the order of the inter-annual variation of the fluxes themselves, thereby inhibiting the full use of these products for certain societal applications. Also, because the land surface exerts a key role in modulating regional fluxes of moisture back to the atmosphere, it is important to constrain uncertainty in surface transfers of energy and moisture to the maximum degree possible. In addition to aforementioned need for improvements in QPE products, critical process-based information is needed on the character of land-atmosphere exchanges across a range of monsoon ecological and physiographic regimes. Watts et al. (2007) and Vivoni et al. (this issue) describe recent progress in observational characterization of land-atmosphere interactions. Advances in these basic areas will help elucidate the nature of the coupling between the land and atmosphere which is, as yet, an unresolved issue as discussed in Bosilovich et al. (2003), Mo and Juang (2003), Zhu et al. (2007), and Dominguez et al. (2008) among others.

Program Synthesis and Remaining Challenges

Although NAME has contributed much in terms of describing the basic regional circulation features of the warm season precipitation over western North America, progress on understanding the role of teleconnective forcing on the monsoon as well as forcing from the NAM on the continental-scale circulation has been comparatively slower. While basic statistical relationships between NAM seasonal precipitation and large-scale mechanisms such as the El Niño-Southern Oscillation (ENSO), the Pacific Decadal Oscillation and, more recently, the Atlantic Multi-decadal oscillation have been established, such relationships tend to be modest in terms of their overall correlation structure and, at times, transient, over climatological periods of record (e.g. Higgins et al., 1998; Hu and Feng, 2008; Gochis et al., 2007b). Similarly, the role of antecedent land surface conditions in modulating seasonal anomalies in monsoon rainfall is not exceptionally well understood to

the degree that it may or may not provide additional skill to seasonal NAM forecasts. The relatively weak correlations and lingering uncertainties that exist with respect to the interplay between the regional climate of the NAM and potential large-scale forcing mechanisms imply a comparatively weakly forced climate regime in which synoptic and mesoscale transients can, and do, play a large role in determining the overall structure of seasonal anomalies (c.f. Douglas and Englehart, 2007). Improved description of the role of transients such as tropical disturbances (as discussed in the articles below by Higgins et al. and Mejia and Douglas), the Madden-Julien Oscillation (e.g. Lorenz and Hartmann, 2006) and mid-latitude wave patterns, is needed to continue advancing medium range and seasonal predictions of monsoon activity.

In recognition of the significant role played by transient (i.e. chaotic) disturbances on the NAM, several groups are pursuing the development of ensemble-based forecasting techniques in both mesoscale and global-scale predictions of NAM rainfall. Recently, Liang et al. (2007) used an optimal ensemble-member selection methodology in a mesoscale model to improve hindcast simulations of rainfall over western Mexico and the southwestern U.S. Maitaria et al. (2008) have been pursuing a blended dynamical-statistical system, in order to optimally-downscale medium-range (14-day), global model forecasts of NAM rainfall for water resources applications. Munoz et al. (this issue) also present initial findings from an ensemble-based hydrologic forecast system for the U.S. and Mexico. These and similar methods are increasingly acknowledged as a means to provide needed improvements to warm season precipitation forecasts while work on making fundamental improvements in model physics, operational observing networks and data assimilation methods continues along in tandem.

As the coordinated, programmatic research efforts under NAME begin to wind down over the next two years, much work remains in order to fulfill NAME's ultimate goal of improving predictions of warm season precipitation. Ultimately, the work accomplished under NAME must contribute to the larger issue of understanding the roles of the American monsoon systems in the global climate system, which is a principal goal of the CLIVAR Variability of American MOonsoon Systems (VAMOS) research program (c.f. Vera et al., 2006). Similarly, the accomplishments of NAME should and will be used as a foundation for developing a newly proposed research effort aimed at improving understanding and prediction of climate variability in the Intra-Americas Seas region (IASCLiP Science Working Group, 2007). Achieving these broader objectives will entail persistent coordination and investment in both observational and modeling infrastructure throughout the Americas. Coordinated networks of climate reference stations across the Americas, such as that proposed by Diamond et al. (2007) and Diaz et al. (2006) need to be implemented and sustained. These networks would capitalize on improvements in telecommunications and sensor technology such as global positioning system (GPS) retrievals of precipitable water vapor described in the article by Kursinski et al. (this issue). Advancement of process-based understanding and prediction skill within these and other CLIVAR programs can then be used to provide an improved physical basis for predicting, understanding and mitigating the impacts of a changing climate on the Americas.

References

- Bosilovich M.G., Y.C. Sud, S.D. Schubert, G.K. Walker, 2003. Numerical simulation of the large-scale North American monsoon water sources. *J. Geophysical Research* **108(D16)**: 8614, doi:10.1029/2002JD003095.

- Ciesielski, P.E. and R.H. Johnson, 2008: Diurnal cycle of surface flows during 2004 NAME and comparison to model reanalysis. In press, *J. Climate*.
- Diaz, H.F., R. Villalba, G. Greenwood and R.S. Bradley, 2006: The impact of climate change in the American Cordillera. *Eos*, Transactions of the American Geophysical Union, **87(32)**, August, 2006, p. 315.
- Diamond, J.J. and M.R. Helfert, 2007: The U.S. Global Climate Observing System (GCOS) Program : Plans for high elevation GCOS surface network sites based on the benchmark U.S. Climate Reference Network (CRN) System. Mountain Views, *Newsletter of the Consortium for Integrated Climate Research in Western Mountains (CIRMOUNT)*, **1**, 16-19.
- Dominguez, F., P. Kumar and E.R. Vivoni, 2008: Precipitation recycling variability and exoclimatological stability- A study using NARR Data. Part II: North American monsoon Region. In press, *J. Climate*.
- Douglas, A.V. and P.J. Englehart, 2007: A climatological perspective of transient synoptic features during NAME 2004. *J. Climate*, **20**, 1947-1954.
- Ek, M.B., K.E. Mitchell, Y. Lin, E. Rogers, P. Grunmann, V. Koren, G. Gayno and J.D. Tarpley, 2003. Implementation of Noah land surface model advances in the National Centers for Environmental Prediction operational mesoscale Eta model. *J. Geophys. Res.*, **108(D22)**, 8851, doi:10.1029/2002JD003296.
- Gebremichael, M., E.R. Vivoni, C.J. Watts, J. Garatuza-Payan and J. Cesar-Rodriguez, 2007: Submesoscale spatiotemporal variability of North American monsoon rainfall over complex terrain. *J. Climate*, **20**, 1751-1773.
- Gochis, D.J., A. Jimenez, C.J. Watts, J. Garatuza-Payan and W.J. Shuttleworth, 2004: Analysis of 2002 and 2003 warm-season precipitation from the North American monsoon Experiment event rain gauge network. *Mon. Wea. Rev.*, **132**, 2938-2953.
- Gochis, D.J., L. Brito-Castillo, and W.J. Shuttleworth, 2006: Hydroclimatology of the North American monsoon region in northwest Mexico. *J. Hydrol.*, **316**, 53-70.
- Gochis, D.J., L. Brito-Castillo, and W.J. Shuttleworth, 2007a: Correlations between sea-surface temperatures and warm season streamflow in northwest Mexico. *Int. J. Climatol.*, **27**, 883-901.
- Gochis, D.J., C.J. Watts, J. Garatuza-Payan, and J. Cesar-Rodriguez, 2007b: Spatial and temporal patterns of precipitation intensity as observed by the NAME event rain gauge network from 2002 to 2004. *J. Climate*, **20**, 1734-1750.
- Gochis, D.J., S. Nesbitt and W. Yu, 2008: Comparison of gauge-corrected versus non-gauge corrected satellite precipitation intensity estimates during the 2004 NAME Enhanced Observing Period. Submitted to *Atmosfera*.
- Gutzler, D.S., H.K. Kim, R.W. Higgins, H.M.H. Juang, M. Kanamitsu, K. Mitchell, K. Mo, P. Pegion, E. Ritchie, J.K. Schemm, S. Schubert, Y. Song and R. Yang, 2005: The North American Monsoon Model Assessment Project: Integrating numerical modeling into a field-based process study. *Bull. Amer. Meteorol. Soc.*, **86(10)**, 1423-1429.
- Higgins, R.W., K.C. Mo, and Y. Yao, 1998: Interannual variability of the U.S. summer precipitation regime with emphasis on the southwestern monsoon. *J. Climate*, **11**, 2592-2606.
- Higgins, R.W. and co-authors, 2003: Progress in Pan-American climate variability research: The North American monsoon system. *Atmosfera*, **16**, 29-65.
- Higgins and co-authors, 2006: The North American Monsoon Experiment (NAME) 2004 field campaign and modeling strategy. *Bull. Amer. Meteor. Soc.*, **87**, 79-94.
- Hong, Y., D.J. Gochis, J.-T. Cheng, K.-L. Hsu, and S. Sorooshian, 2007: Evaluation of PERSIANN-CCS rainfall measurement using the NAME event rain gauge network. *J. Hydrometeorol.*, **8**, 469-482.
- Hu, Q. and S. Feng, 2008: Variation of the North American summer monsoon regimes and the Atlantic Multidecadal Oscillation. In press, *J. Climate*.
- IASCLiP Science Working Group, cited 2007: A Science and Implementation Plan for the Intra Americas Study of Climate Processes (IASCLiP).
- Janowiak, J.E., V.J. Dagostaro, V.E. Kousky, and R.J. Joyce, 2007: An examination of precipitation in observations and model forecasts during NAME with emphasis on the diurnal cycle. *J. Climate*, **20**, 1680-1692.
- Lang, T.J., D.A. Ahijevych, S.W. Nesbitt, R.E. Carbone, and S.A. Rutledge, 2007: Radar-observed characteristics of precipitating systems during NAME 2004. *J. Climate*, **20**, 1713-1733.
- Liang, X.-L. M. Xu, K.E. Kunkel, G.A. Grell, and J.S. Kain, 2007: Regional climate model simulation of U.S.-Mexico summer precipitation using the optimal ensemble of two cumulus parameterizations. *J. Climate*, **20**, 5201-5207.
- Lobato-Sanchez, R., R.W. Higgins, O. Rodriguez-Lopez, F. Oropeza-Rosales, C. Arias-Lopez, I. Mendoza-Uribe, W. Shi, E. Yarosh, and J. Salinas, 2007: A simple rain gauge network in support of NAME. *Oral presentation at the 7th Meeting of the NAME Science Working Group*. Information available online at: (<http://galileo.imta.mx/DBNAME/>).
- Lorenz, D.J. and D.L. Hartmann, 2006: The effect of the MJO on the North American monsoon. *J. Climate*, **19**, 333-343.
- Maitaria, K., S. Mullen, D.J. Gochis, W.J. Shuttleworth and D.N. Yates, 2008: Development of downscaled, medium-range, probabilistic prediction system for the North American monsoon. *Manuscript in preparation*.
- Mo, K.C. and H.-M. H. Juang, 2003: Relationships between soil moisture and summer precipitation over the Great Plains and the Southwest. *J. Geophys. Res.*, **108(D16)**, doi:10.1029/2002JD002952.
- NAME Science Working Group, cited 2008: *North American Monsoon Experiment Science and Implementation Plan*. [Available online at <http://www.cpc.ncep.noaa.gov/products/monsoon/NAME.html>].
- Nesbitt, S.W., D.J. Gochis and T. Lang, 2008: Characteristics of convection along the Sierra Madre Occidental observed during NAME-2004: Implications for warm season precipitation estimation in complex terrain. Submitted to *J. Hydrometeorol.*
- Rowe, A. K., S. A. Rutledge, T. J. Lang, P. E. Ciesielski, and S. M. Saleeby, 2008: Elevation-dependent trends in precipitation during NAME. *Mon. Wea. Rev.*, submitted.
- Vera, C. and co-authors, 2006: Toward a unified view of the American monsoon systems. *J. Climate*, **19**, 4977-5000.
- Vivoni, E.R., H.A. Gutierrez-Jurado, C.A. Aragon, L.A. Mendez-Barrozo, A.J. Rinehart, R.L. Wycoff, J.C. Rodriguez, C.J. Watts, J.D. Bolten, V. Lakshmi and T.J. Jackson, 2007a: Variation of hydrometeorological conditions along a topographic transect in northwestern México during the North American monsoon. *J. Climate*, **20**, 1792-1809.
- Watts, C.J., R.L. Scott, J. Garatuza-Payan, J.C. Rodriguez, J.H. Prueger, W.P. Kustas and M. Douglas, 2007: Changes in vegetation condition and surface fluxes during NAME 2004. *J. Climate*, **20**, 1810-1820.
- Zhu C, T. Cavazos and D. Lettenmaier, 2007: Role of antecedent land surface conditions in warm season precipitation over northwestern Mexico. *J. Climate* **20(9)**: 1774-1791.

Atmospheric simulations of the 2004 North American Monsoon circulation: NAMAP2

Gutzler, D.¹, L. N. Long², J. Schemm³, M. Bosilovich⁴, J. Chern⁵, J. C. Collier⁶, M. Kanamitsu⁶, P. Kelly⁷, D. Lawrence⁸, M.-I. Lee^{4,5}, R. Lobato S.¹², B. Mapes⁷, K. Mo³, A. Nunes⁹, E. Ritchie⁹, J. Roads⁹, S. B. Roy¹⁰, S. Schubert⁴, H. Wei¹¹ and G. Zhang⁶
¹University of New Mexico, ²Wyle Information Systems, ³NOAA Climate Prediction Center, ⁴NASA Goddard Space Flight Center, ⁵University of Maryland/Baltimore County, ⁶Scripps Institution of Oceanography, ⁷University of Miami, ⁸National Center for Atmospheric Research, ⁹University of Arizona, ¹⁰University of Illinois, ¹¹NOAA Environmental Modeling Center, ; ¹²Instituto Mexicano de Tecnología del Agua, Corresponding author: gutzler@unm.edu

1. Introduction

The North American Monsoon system has been an active target for numerical simulation for many years. A coordinated set of retrospective simulations of the 1990 summer season, called the NAME Model Assessment Project or NAMAP, was carried out prior to the NAME field campaign in 2004 (Gutzler et al. 2005). One of the products of the NAMAP set of simulations was a set of goals for model simulation improvement, based on several important features of the seasonal evolution of the NAMS that seemed problematic. These goals were formulated in terms of metrics for subsequent simulations (Gutzler et al. 2005). The metrics included:

- Correct simulation of monthly averaged precipitation rates to within 20% throughout the diurnal cycle.
- Determination of observed monsoon onset to within 1 week.
- Simulation of the magnitude of the observed afternoon peak of latent and sensible heat fluxes to within 20% on a monthly averaged basis.
- Correct simulation of the position of the Gulf of California low-level jet with respect to the Gulf and the high topography to the east.

NAMAP considered only monthly mean output averaged over spatial subregions within NAME Tier I (Figure 1). The present study, denoted NAMAP2, is designed to re-examine the NAMAP metrics in a new coordinated set of simulations of the 2004 warm season, and extend NAMAP's temporal and spatial limitations to consider other NAME-related subregions and sub-monthly temporal variability. Daily resolution is clearly needed to address the NAMAP metric concerning monsoon onset, as well as many other diagnostic quantities of interest.

To some degree, success in achieving these simulation goals is limited by our ability to validate them. The difference between operational precipitation analyses for this period is generally on the order of 10% across much of the area depicted, and in some subregions the difference between observational products approaches 20%, which is the NAMAP-specified metric for successful model simulation. It is quite likely that actual surface fluxes are not known to within 20% across the NAME domain. Likewise, existing analyses of observed precipitation across NAME Tier I do not properly constrain the diurnal cycle. For studies of the diurnal cycle the challenge in validating models with available data involves comparison of pointwise raingauge observations (Gochis et al. 2007) with model-generated gridcell values, although new NAME observations should improve this situation.

The value of NAMAP2, therefore, is not so much in demonstrating that a particular model does or does not capture a quantitative metric of the monsoon, or performs better than other models, for one summer season. Instead this model assessment exercise should be considered a step in an ongoing iterative process of simultaneously improving both modeling capabilities and observational analyses pertaining to the summer climate of southwestern North America. Progress on both fronts will be necessary to achieve NAME's ultimate goal of improving seasonal prediction skill. At this stage of the NAMAP2 analysis we are emphasizing just the spread among models, rather than

attempting to complete a detailed process-based analysis of individual model output.

As we move forward the results of NAMAP2 are being directly fed into operational forecast model development efforts at NOAA's Environmental Modeling Center through the NAME Climate Process Team effort.

2. NAMAP2 Models and Protocols

The NAMAP2 simulation period extends across the boreal warm season of 2004, when the NAME Enhanced Observation Period took place. Some of the NAMAP2 participants were active in the first round of NAMAP simulations. Several other modeling groups volunteered following presentations soliciting participation at NAME science workshops and other scientific meetings. Participants helped to design the modeling strategy and common boundary conditions used in the simulations.

Time-varying SST was the principal prescribed surface boundary condition for NAMAP2 simulations. Experience from the initial NAMAP exercise indicated that existing operational SST products tend to be considerably too cold in the Gulf of California. Some observational evidence (e.g. Mitchell et al. 2002) suggested that proper simulation of surface temperature in the Gulf might be critical for properly simulating sufficiently strong atmospheric moisture transport up the Gulf, although regional models do not consistently reproduce such sensitivity (Mo and Juang 2003). Wang and Xie (2007) created a new SST analysis product for NAMAP2, denoted MPM, that incorporates multiple sources of satellite data to improve the temporal and spatial resolution of the surface temperature field, with special attention given to the Gulf of California. Most of the NAMAP2 simulations used the MPM analysis; one modeling group ran their seasonal simulation twice, once with MPM as the ocean surface temperature boundary conditions and another with an operational SST analysis. No standard was set for land surface models, and each modeling group picked its own land surface component.

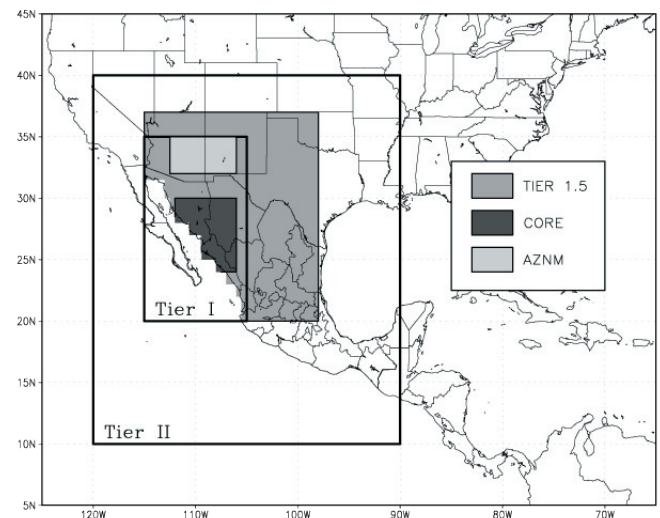


Figure 1: Analysis domains used for defining spatial averages. Tiers I and II are defined in the NAME Science Plan; CORE and AZNM were used in the first round of NAMAP (Gutzler et al. 2005) and are used in NAMAP2 as well; Tier 1.5 is newly defined for NAMAP2.

NAMAP2 simulations were carried out by six global modeling groups and four regional modeling groups (summarized in Table 1; more complete information on the different models can be obtained from the NAMAP2 web page at URL <http://www.eol.ucar.edu/projects/name/namap2>). A key difference between the global and regional model protocols is the constraint provided by prescribed time-varying lateral boundary conditions for the regional models. These boundary values were provided by the AMIP-II reanalysis product (Kanamitsu et al. 2002). Global models generated their own large-scale circulations, constrained by prescribed ocean temperatures. Thus comparing the global and regional model simulations provides a suggestion of the importance of the correct simulation of the large-scale circulation surrounding the monsoon domain, and how well the global models succeed in creating that circulation.

Participating modelers were requested to submit an agreed-upon list of variables with three-hourly resolution for archiving and analysis at the NOAA Climate Prediction Center. Output was submitted over an analysis domain that corresponded to the "Tier II" region (Figure. 1) defined in the NAME Science Plan, which extends across southwestern North America from 10°N to 40°N in latitude, and 90°W to 120°W in longitude. Spatial averages within Tier I (Figure 1) were used for many analysis purposes. Most of the subregions shown in Figure 1 have been used in previous NAME-related diagnostic studies. One new region, Tier 1.5, was defined for this analysis because NAMAP indicated that a common modeling flaw involved generating precipitation too far to the east relative to observations. Tier 1.5 was designed to capture such precipitation.

3. Synopsis of NAMAP2 Simulations of the 2004 North American Monsoon

In this brief synopsis we will focus on the first metric listed in the Introduction, pertaining to the monthly means and diurnal cycle of warm season precipitation, and consider just the CORE subregion (Figure 1). Monsoon onset, surface fluxes, regional low-level jet circulations and other features of the simulations will be described in more detail in a lengthier article now in preparation. An online atlas of NAMAP2 results, hosted at the University of Miami, contains a much more comprehensive set of images of NAMAP2 results. The URL for the NAMAP2 atlas is <http://www.rsmas.miami.edu/personal/pkelly/Research.html>. This site can also be reached via a link from the NAMAP2 webpage at URL <http://www.eol.ucar.edu/projects/name/namap2>.

Time series of three different estimates of total monthly observed precipitation [URD, a gauge-based analysis (Higgins et al. 2000); TRMM, a satellite-based estimate (Huffman et al. 2007); and RMORPH, a prototype satellite-gauge blend (Janowiak

et al. 2007)] from May to September 2004, averaged over the CORE subregion (Figure 2, page 15, black lines), all show the pronounced increase between June and July typical of the North American monsoon. In 2004 CORE precipitation decreased in August relative to July. All the simulations (both global and regional) shown in Figure 2, with one exception, reproduce an increase in total precipitation from June to July. This represents a marked improvement over the NAMAP simulations, for which the global models systematically delayed monsoon onset and thereby misrepresented the seasonal progression. Two of the global model simulations (blue and yellow lines in Figure 2a) stand out as drier in July compared to the other models and observations. These particular simulations initiate precipitation too far to the east; the seasonal progression of precipitation in these two simulations is closer to observations when rainfall is averaged across the larger Tier 1.5 region (not shown). The spread of CORE-average precipitation among global models increased in August, with four models continuing to increase precipitation from July to August, one model initiating its precipitation in August instead of July, and two models following the observed progression of a July peak followed by an August decrease.

All the regional models also simulate a large increase in CORE precipitation from June to July (Figure 2b), and all models except one then properly exhibit a decrease in precipitation from July to August. As was the case in NAMAP, the MM5 simulations (red and light blue lines in Figure 2b) tend to oversimulate precipitation in the CORE subregion.

Most global models simulated the diurnal cycle of total precipitation in the CORE subregion reasonably well, as determined from satellite-based estimates (TRMM or RMORPH), whereas the regional models seem to exhibit much less consistency despite the higher resolution used for these simulations (results for total precipitation are not shown here; see the NAMAP2 atlas). To examine this counterintuitive result in more detail, we considered separately the diurnal cycle of convective precipitation (left panels) and resolved precipitation (right panels) in the CORE subregion for Jun-Aug 2004 (Figure 3, page 15).

The diurnal cycle of convective precipitation (Figure 3, left panels) reaches a peak near 00Z in all models. The amplitude of convective precipitation varies considerably among the global models but is remarkably consistent among the regional models (three of which are represented here; one model was excluded from this comparison because of evident problems with the high-frequency output data set). The rate of resolved precipitation, i.e. rain from grid saturation or fractional cloudiness schemes, is much smaller in global models (note that the y-axis in Fig 3b is greatly expanded relative to the other

Model Name	Affiliation / Contact	Horizontal Resolution	Ensemble Size	SST Prescription
CFS (Operational)	NOAA CPC / Schemm	T126 (~1°)	5	MPM
GFS	NOAA CPC / Mo & Wei	T126	4	MPM
CAM3_a	UCSD SIO / Collier & Zhang	T42 (~2.8°)	1	MPM
CAM3_b	NCAR / Lawrence	1.0°×1.25°	1	Hadley
CAM3_c	UCSD SIO / Collier & Zhang	T42 (~2.8°)	1	Era-40
Finite Volume	NASA GSFC / Bosilovich	0.25°×0.36°	2	MPM
GEOS5	NASA GSFC / Lee & Schubert	0.5°	5	MPM
RAMS	<i>Duke U / Roy</i>	64 km	1	NOAA OI
RSM	UCSD SIO / Nunes & Roads	30 km	1	MPM
MM5_a	IMTA / Lobato	30 km	3	MPM
MM5_b	UNM / Ritchie	15 km	1	MPM

Table 1. Listing of models participating in NAMAP2 and their key characteristics. The six global models are indicated in non-italic type; four regional models in italics.

panels in Figure 3). In contrast, resolved precipitation in the regional models (Figure 3d) is generally of equivalent amplitude to convective precipitation but varies hugely from one model to another. The large amount of resolved precipitation in the MM5 simulations accounts for much of the overestimate of total precipitation by these models noted in Figure 2b.

The results in Figure 3 indicate that the treatment of precipitation, in terms of the overall amplitude and diurnal cycle, is occurring quite differently in the various models. Convective precipitation in these high resolution regional models was reasonably consistent from model to model, despite their use of different convective parameterizations, but the transition to resolved precipitation (several hours after the convective peak) was handled very differently in the various models. The global models generally produced little or no resolved precipitation, so model-to-model differences must have resulted from different treatments of moist convection, and/or from different simulations of flow and thermodynamic structure in the NAM region as part of their different global climates.

4. Concluding Remarks

Ten modeling groups carried out a coordinated set of simulations of the 2004 North American monsoon season. Here we have summarized aspects of precipitation variability in the CORE subregion that had been flagged in the previous NAMAP exercise as worthy of special attention. All models achieved some degree of fidelity in simulating the onset and seasonal evolution of the monsoon and the diurnal cycle of precipitation, but, as expected, there were considerable differences among models in the amounts. A much more complete set of NAMAP2 graphics is freely available in an online atlas, and additional analyses of the results are being prepared for publication.

In addition to the spatially averaged results reported in this paper, a more detailed analysis is being carried out for column model results from these same simulations at model locations that correspond to the sites of NAME intensive observations. The models' moist processes that turn atmospheric moisture into clouds and precipitation are also being examined at these sampled grid columns. Time-height plots of data from these soundings and other sites can be found on the Web atlas.

This component of the NAMAP2 analysis examines the hypothesis that land-atmosphere interaction (LAI) errors in these simulations, as seen in analysis of the diurnal cycle (which is well-sampled within a single field season), may provide clues to their systematic errors in the largely land heating-driven synoptic flow structure of the NAM system. If so, then improving the relevant model physics schemes by diurnal cycle calibration might improve seasonal simulations and forecasts of the synoptic flow and thus moisture fluxes. Land surface observations were a strong point of NAME, so collaborations between atmospheric and hydrology communities will be fruitful, although the upscaling problem is especially daunting in such heterogeneous landscapes.

As we move forward, the results of NAMAP2 are being directly fed into operational forecast model development efforts at NOAA's Environmental Modeling Center through the NAME Climate Process Team effort. As a modeling component of NAME, the overarching goal is to leave a legacy of improved observations, process-based understanding, simulation capability, and ultimately prediction skill for summer climate variability associated with the North American monsoon.

References

Gochis, D.J., C.J. Watts, J. Garatuza-Payan and J. Cesar-Rodriguez, 2007: Spatial and temporal patterns of

precipitation intensity as observed by the NAME event rain gauge network from 2002 to 2004. *J. Climate*, **20**, 1734-1750.

- Gutzler, D.S., H.-K. Kim, R.W. Higgins, H. Juang, M. Kanamitsu, K. Mitchell, K.C. Mo, P. Pegion, E.A. Ritchie, J.-K. Schemm, S.D. Schubert, Y. Song and R. Yang, 2005: The North American Monsoon Model Assessment Project: Integrating numerical modeling into a field-based process study. *Bull. Amer. Meteor. Soc.*, **86**, 1423-1429.
- Higgins, R.W., W. Shi, E. Yarosh and R. Joyce, 2000: Improved United States Precipitation Quality Control System and Analysis. *NCEP/Climate Prediction Center ATLAS No. 7*, 40 pp. [Available from NOAA Climate Prediction Center, 5200 Auth Road, Camp Springs, MD 20746].
- Huffman, G.J., R.F. Adler, D.T. Bolvin, G. Gu, E.J. Nelkin, K.P. Bowman, Y. Hong, E.F. Stocker, and D. B. Wolff, 2007: The TRMM Multi-satellite Precipitation Analysis (TMPA): Quasi-global, multi-year, combined-sensor precipitation at fine scales. *J. Hydrometeorol.*, **8**, 38-55.
- Janowiak, J.E., V.J. Dagostaro, V.E. Kousky and R.J. Joyce, 2007: An examination of precipitation in observations and model forecasts during NAME with emphasis on the diurnal cycle. *J. Climate*, **20**, 1680-1692.
- Kanamitsu, M., W. Ebisuzaki, J. Woolen, S. K. Yang, J. J. Hnilo, M. Fiorina and G. L. Potter, 2002: NCEP/DOE AMIP-II reanalysis (R-2). *Bull. Amer. Meteor. Soc.*, **83**, 1631-1643.
- Mitchell, D.L., D. Ivanova, R. Rabin, T.J. Brown and K. Redmond, 2002: Gulf of California sea surface temperatures and the North American Monsoon: Mechanistic implications from observations. *J. Climate*, **15**, 2261-2281.
- Mo, K.C., and H.M.H. Juang, 2003: Influence of sea surface temperature anomalies in the Gulf of California on North American monsoon rainfall. *J. Geophys. Res.*, **108**, doi:10.1029/2002JD002403.
- Wang, W., and P. Xie, 2007: A Multiplatform-merged (MPM) SST analysis. *J. Climate*, **20**, 1662-1679.



Congratulations to Mike McPhaden recently named as President-elect of the American Geophysical Union (AGU). AGU is the largest organization of professional geophysicists in the world, with over 50,000 members from 137 countries.

Mike is a Senior Scientist and Director of the Tropical Atmosphere

Ocean (TAO) Array Project Office at NOAA's Pacific Marine Environmental Laboratory (PMEL) in Seattle, Washington. He is also an affiliate Professor in the School of Oceanography at the University of Washington. He has had a long association with CLIVAR. He is a member of the Indian Ocean Panel, the Global Synthesis and Observations Panel, the OceanSITES Working Group, an ex officio member of the Pacific Panel and chair of the Tropical Moored Buoy Implementation Panel. He was also a contributing author to the IPCC fourth assessment report.

Mike will serve for two years as President-elect of AGU beginning in July 2008 and will then become President for two years in July 2010.

Relationships between Gulf of California moisture surges and tropical cyclones in the Eastern Pacific Basin

R. W. Higgins, W. Shi and K. C. Mo
Climate Prediction Center, NOAA/NWS/NCEP, Washington, D.C., USA
Corresponding author: Wayne.Higgins@noaa.gov

Motivation

Northward surges of relatively cool, moist maritime air from the eastern tropical Pacific into the southwestern United States via the Gulf of California (GoC) are strongly related to the amount of convective activity and precipitation in the region during the summer monsoon. These events, referred to as "moisture surges", are often related to the passage of Tropical Cyclones (TCs) south of Baja California. This study documents the atmospheric circulation, GoC sea surface temperatures, and moisture and precipitation patterns that accompany these events, with emphasis on the relative differences in these patterns for several categories of surge events, including those that are directly related to TCs, indirectly related to TCs and not related to TCs. It is shown that roughly half of all GoC moisture surges are influenced by TCs (Table 1).

Results

The response to moisture surges in northwestern Mexico and the southwestern U.S. is strongly discriminated by the presence or absence of TCs. Surges that are directly related to TCs tend to be associated with much stronger and deeper low-level southerly flow, deeper plumes of tropical moisture, and wetter conditions over the core monsoon region than surges that are unrelated to TCs (Figure 1, page 16). The response to the surge is also strongly influenced by the proximity of the TC to the GoC region. TCs that track in close proximity to the

Category	Number of Events
All	132
TC-Related	65 (49%)
Not Related to TCs	67 (51%)
Direct	38 (58% of TC-related)
Indirect	27 (42% of TC-related)

Table 1. Number (fraction in percent) of total surge events at Yuma, AZ that were TC-related and not TC-related during the period July-August 1979-2001. Yuma surges are further subdivided into those with direct (indirect) relationships to TCs.

GoC exert a stronger, more direct influence on moisture surges than those that track away from the GoC. Even when directly influenced by TCs, the response to the surge in the southwestern U.S. depends strongly on the location of the upper-level monsoon anticyclone in midlatitudes at the time of the surge. In particular, when the anticyclone is centered to the east of the four-corners region (i.e. the intersection of Arizona, New Mexico, Colorado and Utah), wetter-than-normal conditions often occur in Arizona and New Mexico. Alternately, when the anticyclone is centered near the west coast, drier-than-normal conditions often occur.

While the SSTs in the GoC do not influence the surge events, the TC related surge events often cool the SSTs in the GoC. These surge events are usually accompanied by enhanced cloudiness that prevents short wave radiation from reaching the surface. As a consequence, the net radiation entering the ocean decreases leading to the cooler SSTs.

Ramifications and Future Work

Moisture surges, TCs and their relationships are important components of the North American monsoon system that must be understood in order to improve simulations and predictions of warm season precipitation with coupled climate models. In an effort to understand features such as these, the North American Monsoon Experiment (NAME) Program carried out a major field campaign in southwestern North America during June-September 2004. An unprecedented set of *in situ*, sounding, radar, aircraft and remote sensing data were gathered during the campaign. These data are being used to produce high resolution global and regional atmospheric analyses for NAME data impact studies that elucidate the influence of the regional monsoon circulation on the larger scale during moisture surge events. This includes studies of the influence of the leading sources of climate variability (such as El Niño-Southern Oscillation and the Madden-Julian Oscillation) on TC-surge-precipitation relationships. The NAME 2004 data are also being used by the global and regional modeling communities to evaluate our ability to simulate (and ultimately predict) the characteristics of surges, such as those emphasized here.

Relationship of TEWs and spatial-temporal variability of MCSs in the North American Monsoon Region

Mejia, J¹. and M Douglas²

¹Cooperative Institute for Mesoscale Meteorological Studies /University of Oklahoma, Norman, Oklahoma, ²National Severe Storms Laboratory/NOAA, Norman, Oklahoma

Corresponding author: Michael.Douglas@noaa.gov

Abstract

This study is focused on the spatial, seasonal and interannual variability of Mesoscale Convective Systems (MCSs) as a function of Tropical Easterly Waves (TEWs) affecting the North American Monsoon System (NAMS). First, MCSs are characterized by their cloud shield signatures using 10 km infrared geostationary satellite data with three-hourly time resolution. A survey of multiyear occurrence (from 1990 to 2006) of MCSs is then performed and subsequently correlated with synoptic-scale TEW disturbances. The North American Regional Reanalyses (NARR) are used to characterize the atmospheric disturbances and the overall circulation of the TEWs. The relationship between TEWs and MCSs helps to diagnose the MCS forcing on synoptic time-scales. Comparing active and inactive periods of TEWs shows promise for

explaining rainfall variations over the NAMS domain.

1. Introduction

The effect of Tropical Easterly Waves (TEWs) during the North American Monsoon (NAM) has been long alluded to (Hales, 1972; Brenner, 1974). Although there are other sources of variability for NAM rainfall, acting over a wide range of space and time scales, a considerable part of this variability is linked to fluctuations in the TEW activity (Fuller and Stensrud, 2000; Douglas and Leal, 2003; Higgins et al., 2004; Adams and Stensrud, 2007; Lang et al., 2007). In the present study, we are investigating the role of TEWs in modulating Mesoscale Convective System (MCS) variability.

It is clear that large-scale synoptic patterns and terrain-induced features play an important role in determining whether MCSs

will occur (McCollum et al., 1995). TEWs are associated with occurrence of Gulf of California (GoC) moisture surges (gulf surges) that in turn provide enhanced low-level moisture flux with strong influence on the convective activity in the NAMS core region (Fuller and Stensrud, 2000; Anderson et al., 2000; Douglas and Leal, 2003; Higgins et al. 2004). Additionally, it has been argued that TEWs also provide a large-scale environment that modifies the rainfall fields in the NAMS core region (Douglas and Leal, 2003; Higgins et al. 2004; Adams and Stensrud, 2007; Lang et al., 2007). For example, using model simulations, Adams and Stensrud (2007) found suggestive results about the role of TEWs on the precipitation fields. Their sensitivity test included comparing two sets of runs (of four one-month periods), with and without filtering TEWs out of boundary conditions. Adams and Stensrud (2007) found that TEWs not only are associated with increased southeasterly low-level moisture flux within the GoC but also redistribute rainfall amounts with no apparent increase in rainfall over the NAMS core region. On the other hand, using radar data from the North American Monsoon Experiment (NAME; Higgins et al., 2006), Lang et al. (2007) stratified different organized convective activity regimes over the southern NAMS core domain that were well correlated with the proximity of TEWs. Among many interesting results, such as characterization of the diurnal cycle for different rainfall regimes and the typical movement of organized convective systems (e.g. MCSs), they concluded that the perturbed environment provided by TEWs is linked with the upscale development of MCSs that in turn contribute about 75% of the total seasonal rainfall amount.

The role that TEWs have in the NAMS core region, in particular their initiation of MCSs, is not well-understood. Some reasons that make this task difficult include: i) the complicated dynamics of the TEWs as they interact with the complex terrain over Central America and Mexico (Zehnder, 2004 and references therein); ii) the marked diurnal cycle of convection (Higgins and Gochis, 2007 conference preprint; Lang et al., 2007); iii) the

possible initiation and modulation of moisture surges (Fuller and Stensrud, 2000; Douglas and Leal, 2003; Higgins et al., 2004); iv) the scarcity of upper-air observations in the region; and v) relatively large sensitivity of model simulations to convective parameterization (Gochis et al., 2002).

In this climatological study, satellite data from the International Satellite Cloud Climatology Project (ISCCP) available from 1983 and the NCEP North American Regional Reanalysis (NARR) are used to identify the principal mechanisms that force or maintain the MCSs on synoptic time-scales and assist in the identification of more localized forcings.

2. Data and Methodology

MCS classification

The identification of MCS events is based on ISCCP infrared (IR) satellite data (Knapp, 2004: ISCCP B1U <http://www.ncdc.noaa.gov/oa/rsad/gibbs/gibbs.html>). The temporal resolution of the radiance data is three-hourly (available since 1983), and the spatial resolution is ~ 10 km at nadir. The MCS identification procedure, a modified version of the Maddox (1980) approach, requires first finding detectable deep convection based on a minimum cloud-top temperature threshold. An IR cloud-top temperature threshold of -52°C is used in order to detect high, potentially precipitating clouds. This procedure cannot exclude non-precipitating cirrus cloud. An MCS is identified when the area of this cold region exceeds $50,000$ km² (approximately). Additionally, the cold cloud mass must be tracked for at least two consecutive images in order to be considered an MCS. The center of the cold cloud mass is identified as the location of the MCS. Although the available observations eventually will permit the study to cover the period from 1983 to the present, only preliminary results for 1990-2006 are shown here.

TEW classification

The daily NCEP NARR (Mesinger et al., 2006) wind, temperature, geopotential height, and specific humidity are used to examine the mean atmospheric environment associated with TEWs (e.g., TCs, inverted troughs, MCSs).

TEWs were automatically tracked by following clusters of positive relative vorticity maximum using NARR wind data at 650 hPa. This procedure helps to track TEWs coming from the Caribbean and others that develop over the eastern coast of Mexico. TEW events were selected only when TC events (U.S. National Hurricane Center data) were absent in the region (at least not closer than 1000 km from the GoC entrance). This technique does not capture all TEW disturbances. For example, multiple centers of vorticity maximum were also tracked westward from the GoM but they did not show coherent spatial structure. Therefore, the automatic TEW selection technique filters these features out while preserving the strongest and most coherent vorticity structures.

3. Relationship between TEWs and MCSs

Figure 1 shows a 15-year analysis of MCS events associated with TEW passage over the NAMS core region. The NAMS core region is divided in two subregions at 25°N to separate the western hills of the Sierra Madre Occidental (SMO) mountains and GoC coastal plains into "northern" and "southern" domains (see domain location in Figure 2a). The co-occurrence of MCSs with TEWs is quantified using the information of trough passages over western Mexico obtained from the NARR daily meridional wind signal at 650 hPa. Figure 1a shows a lagged-time analysis, from -3 days to $+3$ days (lag 0 days indicates the trough axis passage over meridian 105°W), of the mean meridional wind anomaly associated with the trough axis passage calculated at 650 hPa, over meridian 105°W and different latitudinal bands ($15, 20, 25, 30^{\circ}\text{N}$). Only those westward propagating variations in the meridional wind

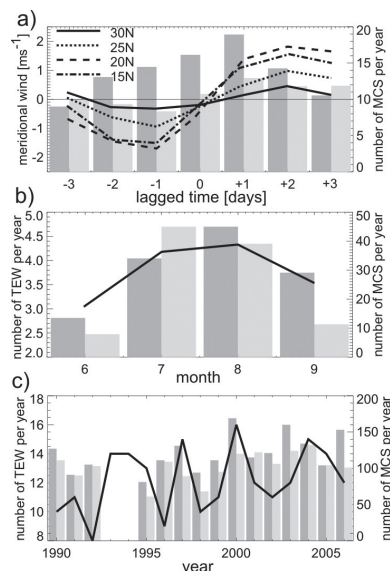
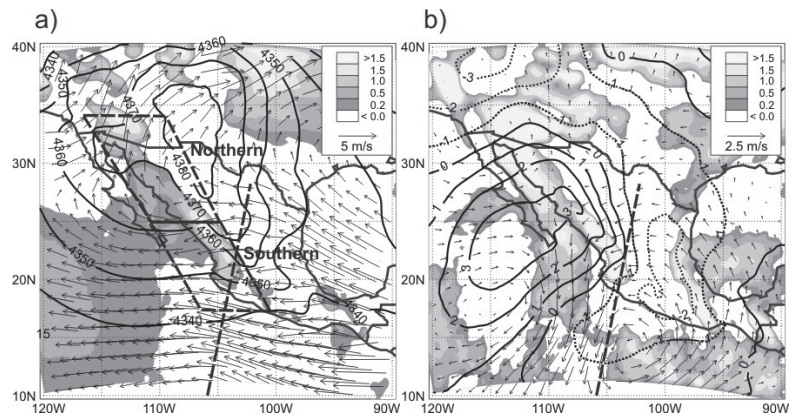


Figure 1 Relationship between TEW activity and MCS events over the NAMS core regions, dark (light) grey for southern (northern) regions (see Figure 2a). a) lagged-time analysis about TEW passage of meridional wind anomaly at 650 hPa for different latitudinal bands (lines; left axis) and occurrences of MCS for regions 1 and 2 (bars; right axis). b) monthly mean number of TEWs (solid line; left axis) and MCS events (bars; right axis). c) annual number of TEWs (solid line; left axis) and MCS events (bars; right axis); totals are for the June-September period.

Figure 2 a) Mean thickness (850-500 hPa; solid contours [m]), mean wind in the layer (arrows [$m s^{-1}$]), and advection of thickness by the wind (shaded areas for positive thickness advection [$1 \times 10^{-4} m s^{-1}$]) for $t=0$ days about the TEW trough axis (dashed line) at 650 hPa; dashed boxes show the northern and southern domains of the NAMS core region referenced in Figure 1. b) same as a) but for anomalies from the mean over the period -3 to +3 days for $t=0$ days (solid (dotted) contours for positive (negative) thickness anomalies [m] and shaded areas for positive thickness advection anomalies [$1 \times 10^{-5} m s^{-1}$]).



associated with synoptic time-scales disturbances crossing over western Mexico were chosen as TEW events (a total of 205 events). Not surprisingly, the meridional wind composites show a change of sign associated with the trough passage with a relatively large meridional extension.

Figure 1a also shows a lagged-time analysis of MCS occurrence about the TEW trough passage. The striking feature here is that significant changes in the number of MCS are observed during the TEW passage. The number of MCSs in the southern domain doubles, from an average of nine MCSs on day -3 to 18 MCSs on day +1, whereas the northern domain only shows an increase of ~60% in the number of MCS - from eight MCSs on day -1 to 13 MCSs on day +1. The maximum number of MCSs events occurs one day after (+1 day) the trough axis passage with relatively more MCS events taking place over the southern domain.

Figures 1b and 1c show the mean seasonal cycle and interannual variability of the TEW activity and how these are related with the MCS activity. The very marked seasonal cycle of MCS activity contrasts with the lesser, though still evident, seasonal change in the TEW activity. While the mean MCS activity doubles in the southern domain and quadruples in the northern domain from June to July, the mean number of TEWs only changes from 3 to 4-4.5 during the same period. This suggests that there are other large-scale features that modulate MCS activity besides TEWs, such as the mean environment - which markedly changes during the late June monsoon onset.

Our results also show considerable interannual variability in both the TEW and MCS activity (Figure 1c). A close examination of Figure 1c for both NAMS core subregions show some level of correspondence between the TEW and the MCS activity for much of the time series. However, a simple linear correlation coefficient between these time series is just 0.29 and 0.43 (considering only 15 years in the time series) for the southern and northern subregions, respectively.

4 Environmental Precursors of MCS

A composite evolution for vertical velocity (ω) using the NARR data indicates that there is an enhanced region of ascent over the NAMS core region associated with the TEW passage over western Mexico (not shown), which is in turn associated with an increase of MCS activity and enhanced cloudiness. However, we sought to determine the large-scale forcing responsible for the enhanced ascent (convective activity). Here, the framework for diagnosis has been the quasi-geostrophic (QG) omega equation by evaluating its forcing terms, thermal advection and differential vorticity advection, in a qualitative sense.

Thermal advection: Figure 2a shows the mean thickness, thickness advection, and wind vectors fields calculated in the atmospheric layer between 850 and 500 hPa at $t=0$ (trough axis over $105^\circ W$).

At this time, northwest Mexico, including the SMO foothills and GoC coastal plains, mostly shows positive thickness (temperature) advection (or warm air advection - WAA) located downstream of the trough axis. Figure 2b shows anomalies of the quantities shown in Figure 2a for day $t=0$ compared to the period -3 to 3 days. The anomaly fields evidence that WAA is accentuated ahead of the trough axis, also observed for days -1 and +1, with a westward propagating motion (not shown). Thus, thermal advection as diagnosed by the Q-G theory acts in favor, in the qualitative sense, to explain ascending motion, hence, favoring the upscale development of MCS. However, for days +2 to +3, to the south of the GoC entrance cold air advection (CAA) dominates and is associated with enhanced southeasterly flow upstream of the trough axis advected from the E. Pacific; congruently, heights fall.

Differential (relative) vorticity advection: Figure 3a (page 12) shows the vorticity, vorticity advection, and mean wind vectors fields calculated at 500 hPa at day $t=0$. This figure shows a coherent region of maximum positive (cyclonic) vorticity advection (PVA) upstream the TEW trough axis (day 0) propagating westward -not shown- over the southern GoC region. This region of PVA becomes more pronounced at day 0 according to the anomaly (Figure 3b) calculated about the period -3 to +3 and it is also co-located with differential PVA -not shown- increasing with height. This feature implies ascending motion from the vorticity advection forcing term and contributes in the same sense as the thermal advection term (WAA co-located in space and time). On the other hand, negative (anticyclonic) vorticity advection (NVA) is coherently observed over NW Mexico (northern GoC and northern SMO foothills) throughout the TEW passage favoring descending motion, which seems to act in the opposite sense as the thermal advection term.

5 Summary and remarks

The analysis presented here, based on the NARR products, suggests that large-scale forcings associated with the TEW play an important role in the organized convective activity in the region.

The QG omega equation and its forcing terms seem to explain qualitatively the enhanced ascent induced by the TEW activity over the E. Pacific and southern GoC. However, the same cannot be said for the northern GoC, where low-level thermodynamic changes (associated with enhanced low-level southeasterly moisture flux, not shown) may be more important in modulating convection. We anticipate that further analysis will improve our understanding of the links between the variability of convection and synoptic forcing over the region.

Acknowledgement

NOAA former OGP and now CPPA sponsored this work through a NAME to MD grant. Thanks are extended to Ken

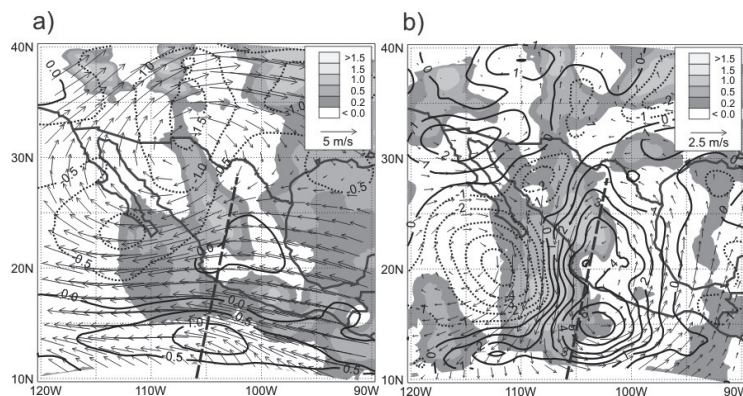


Figure 3 a) vertical component of relative vorticity (500 hPa; solid (dotted) contours for positive (negative) relative vorticity [$1 \times 10^{-5} \text{ s}^{-1}$]), mean wind in the layer (arrows [m s^{-1}]), and advection of vorticity by the wind (shaded areas for positive vorticity advection [$1 \times 10^{-9} \text{ m s}^{-2}$]) on day $t=0$ about the TEW trough axis (dashed line) at 650 hPa. b) same as a) but for anomalies from the mean over the period -3 to +3 days for day $t=0$ (solid (dotted) contours for positive (negative) vorticity anomalies [m] and shaded areas for positive vorticity advection anomalies [$1 \times 10^{-10} \text{ m s}^{-2}$]).

Knapp from NCDC who is facilitating the ISCCP products.

References

- Adams, J. L., D. J. Stensrud, 2007: Impact of tropical easterly waves on the North American monsoon. *J. Climate*, **20**, 1219–1238.
- Anderson B. T., J. O. Roads, and S.-C. Chen, 2000: Large-scale forcing of summertime monsoon surges over the Gulf of California and southwestern United States. *J. Geophys. Res.*, **105**, 24455–24467.
- Brenner I. S., 1974: A surge of maritime tropical air—Gulf of California to the southwestern United States. *Mon. Wea. Rev.*, **102**, 375–389.
- Douglas M.W., and Leal J.C., 2003: Summertime surges over the Gulf of California: Aspects of their climatology, mean structure, and evolution from radiosonde, NCEP reanalysis, and rainfall data. *Weather and Forecasting*, **18**, No. 1 pp. 55–74.
- Fuller, R. D., and D. J. Stensrud, 2000: The relationship between easterly waves and surges over the Gulf of California during the North American monsoon. *Mon. Wea. Rev.*, **128**, 2983–2989.
- Gochis D. J., W. J. Shuttleworth, and Z.-L. Yang, 2002: Sensitivity of modeled North American monsoonal regional climate to convective parameterization. *Mon. Wea. Rev.*, **130**, 1282–1298.
- Hales J. E., 1972: Surges of maritime tropical air northward over the Gulf of California. *Mon. Wea. Rev.*, **100**, 298–306.
- Higgins RW, Shi W, and Hain C, 2004: Relationships between Gulf of California Moisture Surges and Precipitation in the Southwestern United States. *J. Climate*, **17**, 2983–2997.
- Higgins, W., D. and others, 2006: The NAME 2004 Field Campaign and Modeling Strategy. *Bull. Amer. Meteor. Soc.*, **87**, 79–94.
- Higgins, R. W. and D. J. Gochis, 2007: Multi-scale Interactions During the North American Monsoon, Symposium on Connections Between Mesoscale Processes and Climate Variability, *AMS 87th annual meeting*.
- Knapp, K. R., 2004: ISCCP B1 Data at NCDC: A new climate resource. *13th Satellite Meteorology and Oceanography Conference*, Norfolk, VA, American Meteorological Society.
- Lang, T.J., D.A. Ahijevych, S.W. Nesbitt, R.E. Carbone, S.A. Rutledge, and R. Cifelli, 2007: Radar-observed characteristics of precipitating systems during NAME 2004. *J. Climate*, **20**, 1713–1733.
- Maddox, R. A., 1980: Mesoscale convective complexes. *Bull. Amer. Meteor. Soc.*, **61**, 1374–1387.
- McCollum, D.M., R.A. Maddox, and K.W. Howard, 1995: Case Study of a severe mesoscale convective system in Central Arizona. *Wea. Forecasting*, **10**, 643–665.
- Mesinger F, DiMego G, Kalnay E, Mitchell K, Shafran PC, et al., 2006: North American Regional Reanalysis. *Bull. Amer. Meteor. Soc.*, **87**, 343–360.
- Zehnder J. A., 2004: Dynamic mechanisms of the Gulf surge. *J. Geophys. Res.*, **109**, D10107, doi:10.1029/2004JD004616.

Radar-based studies of convection in NAME

Rowe, A. K., S. A. Rutledge, and T. J. Lang
 Department of Atmospheric Science, Colorado State University, Fort Collins, Colorado
 Corresponding author: arowe@atmos.colostate.edu

1. Introduction

The local topography of the core North American Monsoon region in northwestern Mexico is dominated by the Sierra Madre Occidental (SMO), which has been shown to influence the diurnal cycle of monsoon precipitation (e.g., Gochis et al. 2004, 2007; Lang et al. 2007). This diurnal trend is characterized by the initiation of convection over the highest peaks and foothills of the SMO during the late afternoon and a maximum in early morning convection over the lower terrain (e.g., Gochis et al. 2004). Further information on the temporal and spatial variability of precipitation in this region is necessary to improve modeling and forecasting of the North American Monsoon. During the 2004 field component of the North American Monsoon Experiment, a multi-radar network operated in the core monsoon region (Tier I), providing not only improved spatial resolution of precipitation, but also allowing for analysis of vertical characteristics of convection.

2. NAME radar network

This network consisted of the National Center for Atmospheric Research (NCAR) S-band polarimetric Doppler radar (S-Pol), located along the Gulf of California coast (23.93°N , 106.95°W), and two Mexican weather service C-band Doppler radars: Guasave, located north of S-Pol along the coast (25.57°N , 108.46°W), and Cabo, located at the tip of the Baja peninsula (22.89°N , 109.93°W). S-Pol included a set of low-angle 360° surveillance scans for rain mapping, as well as full volume scans extending to higher elevation angles for analysis of the vertical structure of precipitation; both the Cabo and Guasave radars operated only at a single elevation angle. A considerable amount of quality control was applied to data from all three radars; further details regarding the quality control of this data set can be found at http://radarmet.atmos.colostate.edu/name/composites/readme_NAME_regional_radar_composites_v2.pdf. Sweep files from the lowest elevation scans

were then combined to create composites of near-surface rain rate and reflectivity available every 15 minutes from 8 July 0000 UTC through 21 August 2345 UTC on a 0.02° latitude/longitude grid. A three-dimensional data set was created using only S-Pol data to allow for examination of the vertical structure of precipitating features. This information was available at the same temporal and spatial resolution as the 2-D composites, extending to 20 km AGL. The polarimetric variables available from this data set include horizontal reflectivity, differential reflectivity, specific differential phase, linear depolarization ratio, and correlation coefficient.

3. Hourly rainfall statistics

The elevation-dependence of the diurnal cycle of precipitation was investigated by dividing the 2-D rain rate composites into four elevation groups: over water, 0-1000 m (MSL), 1000-2000 m, and greater than 2000 m, based on topographic data available at the same resolution. Figures 1a,b show the hourly median rain rates and precipitation frequency, respectively, as a function of topography and local daylight time (LDT). These plots reveal a trend consistent with results from the NAME Event Rain gauge Network (NERN; Gochis et al. 2004) with convection initiating over the SMO during the afternoon, and less frequent, but more intense convection occurring later over the lower elevations. More specifically, precipitation occurs most frequently at 1600 LDT over the SMO (Figure 1b), reflecting the initiation of afternoon convection over the high peaks and western slopes of the SMO. The highest frequencies continue to be associated with precipitation over the western slopes of the SMO (1000-2000 m) as the day progresses and is characterized by the greatest median rain rates until after 0200 LDT when precipitation is most intense and frequent over the coastal plain (0-1000 m). Lang et al. (2007) concluded that this late night-early morning maximum in precipitation along the coast is primarily due to organized convective systems that propagate westward off the SMO, referred to as Regime A events. Radar data also allowed for classification of two other precipitating regimes: Regime B, corresponding to northward/coast-parallel movement of systems, and Regime AB, the occurrence of both A and B, which, in addition to Regime A, are likely related to enhancement of low-level shear. Further understanding of the impact of environmental factors on organization of precipitating systems,

including interactions with land/sea-breezes, is a topic of future research.

4. Vertical characteristics of precipitation

Vertical characteristics of precipitation as a function of terrain were analyzed to determine possible explanations for the greater rain rates observed at lower elevations compared to the high terrain of the SMO. The 3-D data set from S-Pol was subjected to a convective-stratiform partitioning algorithm based on Yuter and Houze (1997, 1998) to investigate vertical trends in reflectivity for convection specifically. Vertical profiles of reflectivity (not shown) reveal a tendency for convection to be more vertically intense over the lower terrain than over the SMO. Reflectivity profiles were also used to investigate echo-top height distributions as a function of terrain (Figure 1c). Over land and water, peaks in echo-top height at 5 km, 9 km, and 12 km are observed, displaying a trimodal structure similar to that found in Johnson et al. (1999) over the W. Pacific ocean. This structure has been linked to layers of enhanced stability present in the atmosphere that limit vertical growth of convection (Johnson et al. 1999), which were also observed in this study using the CSU-NAME upper-air analyses (Johnson et al. 2007).

The peak at 12 km appears to be absent over the SMO (Figure 1c), indicating the tendency for convection over the higher terrain to be shallower than over the coast. Although the echo-top heights over the lower terrain are higher than over the SMO, this does not necessarily explain the observed trend in rainfall intensity with respect to terrain. The CSU-NAME upper-air and surface analyses were used to calculate the average warm-cloud depth for the elevation groups to investigate potential differences in the depth over which warm-rain processes occur, and the role these differences may contribute to controlling peak rainfall intensity. As was hypothesized, there is a decreasing trend in warm-cloud depth with increasing elevation, reflecting the shallower convection over the SMO compared to the lower terrain. Simulated maximum precipitation intensities with varying warm-cloud depths, using a simplified model of stochastic droplet growth from the CSU RAMS microphysics algorithm described in Saleeby and Cotton (2004), revealed a trend of increasing rainfall intensity with increasing warm-cloud depth (decreasing elevation). This simulated result corresponds with observations, suggesting that the differences in warm-cloud depth between elevation groups could explain the differences in rainfall rates observed by the radar network with respect to elevation. In addition to analysis of warm-rain processes, polarimetric data collected from S-Pol during NAME can be used to provide further details regarding the microphysical variability of convection as a function of terrain.

5. Polarimetric analysis

The 3-D gridded polarimetric data from S-Pol during NAME have been analyzed following the methodologies of Carey et al. (2001) and Cifelli et al. (2002). The behavior of the polarimetric measurands and their derivatives have been examined for four different terrain bands: over water, land 0-500 m, 500-1500 m, and 1500+ m MSL. In general the largest differences occurred between land and sea rather than within different land elevation bands. For example, in high reflectivities (i.e., heavy rain), there were smaller median drop diameters (D_0) and lower differential reflectivities (Z_{DR}) over water than over land (Figure 2, page 16). However, there were few differences in these parameters between the different land elevation bands. Vertical analyses show that precipitation-sized ice mass was similarly smaller over water than over land, while few differences existed between the different land elevation bands. This suggests

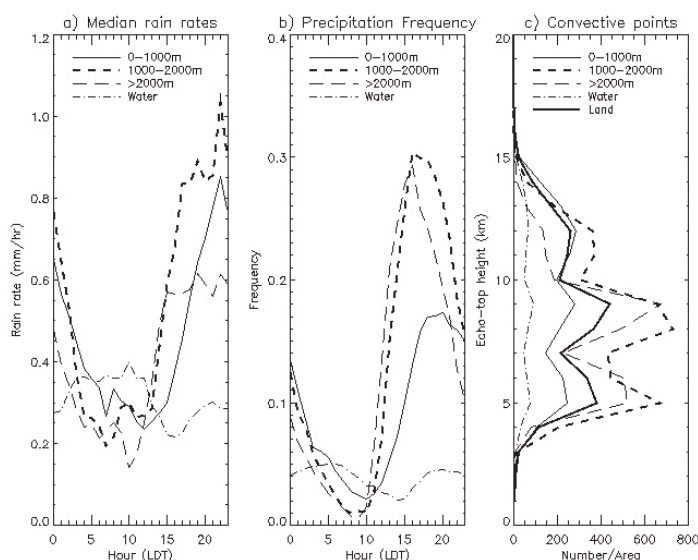


Figure 1. From the 2-D rain rate composites, a) hourly median rain rates, and b) precipitation frequency, normalized by raining and non-raining points. From the 3-D S-Pol data, c) occurrence of convective echo-top heights as a function of elevation.

that fundamental microphysical differences occurred between precipitating systems over land and those over the Gulf of California. Specifically, the results are consistent with the hypothesis that precipitation over water was less dependent on ice-based precipitation processes and more dependent on warm-rain processes, leading to smaller D_0 values and less precipitation-sized ice over the Gulf. In addition, the diurnal cycles of D_0 and other polarimetric measurands were ~12h out of phase between land and sea, consistent with the rainfall results of Lang et al. (2007). These distinct microphysical and meteorological differences between land and sea precipitation during NAME are the focus of ongoing research.

6. Acknowledgements

Radar observations and analyses were funded by the National Oceanic and Atmospheric Administration Grant NA17RJ1228 and the National Science Foundation Grant ATM-0340544.

7. References

- Carey, L. D., R. Cifelli, W. A. Petersen, and S. A. Rutledge, 2001: Characteristics of Amazonian rain measured during TRMM-LBA. Preprints, 30th International Radar Conference, American Meteorological Society, Munich, Germany, 19-24 July, 2001.
- Cifelli, R., W. A. Petersen, L. D. Carey, S. A. Rutledge, and M. A. F. Silva Dias, 2002: Radar observations of the kinematic, microphysical, and precipitation characteristics of two MCSs in TRMM-LBA. *J. Geophys. Res.*, **107**, 10.1029/2000JD0000264.
- Gochis, D. J., A. Jimenez, C. J. Watts, J. Garatuza-Payan, and W. J. Shuttleworth, 2004: Analysis of 2002 and 2003 warm-season precipitation from the North American Monsoon Experiment event rain gauge network. *Mon. Wea. Rev.*, **132**, 2938–2953.
- Gochis, D. J., C. J. Watts, J. Garatuza-Payan, and J. Cesar-Rodriguez, 2007: Spatial and temporal patterns of precipitation intensity as observed by the NAME event rain gauge network from 2002 to 2004. *J. Climate*, **20**, 1734–1750.
- Johnson, R. H., T. M. Rickenbach, S. A. Rutledge, P. E. Ciesielski, and W. H. Schubert, 1999: Trimodal characteristics of tropical convection. *J. Climate*, **12**, 2397–2418.
- Johnson, R. H., P. E. Ciesielski, B. D. McNoldy, P. J. Rogers, and R. K. Taft, 2007: Multiscale variability of the flow during the North American Monsoon Experiment. *J. Climate*, **20**, 1628–1648.
- Lang, T. J., D. A. Ahijevych, S. W. Nesbitt, R. E. Carbone, S. A. Rutledge, and R. Cifelli, 2007: Radar-observed characteristics of precipitating systems during NAME 2004. *J. Climate*, **20**, 1713–1733.
- Saleeby, S. M., and W. R. Cotton, 2004: A large droplet mode and prognostic number concentration of cloud droplets in the Colorado State University Regional Atmospheric Modeling System (RAMS). Part I: Module descriptions and supercell test simulations. *J. Appl. Meteor.*, **43**, 182–195.
- Yuter, S. E., and R. A. Houze Jr., 1997: Measurements of raindrop size distributions over the Pacific warm pool and implications for Z–R relations. *J. Appl. Meteor.*, **36**, 847–867.
- Yuter, S. E., and R. A. Houze Jr., 1998: The natural variability of precipitating clouds over the western Pacific warm pool. *Quart. J. Roy. Meteor. Soc.*, **124**, 53–99.

GPS observations of precipitable water and implications for the predictability of precipitation during the North American Monsoon

Kursinski¹, E. R., D. K. Adams², M. Leuthold¹

¹Department of Atmospheric Sciences, University of Arizona, Tucson, Arizona; ²UEA/INPA, Programa do Clima e Ambiente, Manaus, Brazil
Corresponding author: kursinsk@atmo.arizona.edu

I. Introduction:

The semi-arid to arid North American Southwest has experienced, in recent decades, tremendous population growth despite limited water supplies. Water availability is highly susceptible to climate variability and change and is therefore of great concern. Climate models generally predict the region will experience warmer and drier winters in the future. During summer, incursions of moist tropical air associated with the North American Monsoon (NAM) bring critical convective precipitation (eg. Adams and Comrie, 1997; Higgins et al., 2006). Representing deep convective regimes in tropical regions, however, has been problematic in large-scale numerical models (e.g., general circulation models (GCMs)). The NAM, no exception, is represented poorly, if at all, in GCMs (e.g. Lee et al., 2007). As a result, the future behavior of the monsoon is uncertain but may intensify if the land-sea temperature contrast increases. To improve upon this situation, the North American Monsoon Experiment (NAME) was initiated to better understand convective precipitation and its predictability during the NAM and ultimately improve its modeling. This goal is challenging given the complex interplay between moisture, diurnal heating, large and small-scale dynamics and complex terrain in convective rainfall. Results from data gathered during the 2004 NAME field campaign are briefly summarized here and new results assessing precipitation sensitivity to precipitable water vapor in high resolution model simulations are reported.

Since precipitation condenses from water vapor, improving precipitation prediction requires better knowledge of the

quantity and distribution of water vapor. As such, water vapor was the focus of the International H₂O Project (IHOP) campaign to gain insight into moist convection in the U.S. Southern Great Plains (Weckworth et al., 2004). Like other remote tropical regions, observing water vapor in the NAM region, particularly Mexico, is challenging. During the monsoon, satellite IR observations of water vapor are limited due to frequent cloudiness and microwave water vapor observations in the region are limited due to uncertainties in land surface emissivity. Radiosondes, somewhat intermittent, are found only in Empalme, Mazatlan and La Paz along the Gulf of California coast, Chihuahua, east of the Sierra Madre Occidental (SMO) mountains and Tucson to the north.

II. Key NAME 2004 results

To improve water vapor observations, we fielded an array of GPS receivers and surface meteorological instrumentation at six locations extending from Hermosillo, Sonora to the west to Creel in Chihuahua to the southeast during the 2004 NAME observing period. Precipitable water vapor (PWV) can be derived from GPS receiver measurements to about 1.5 mm (1-sigma) accuracy (Kursinski et al., 2008) in clear and cloudy weather. The GPS receiver and surface instrumentations are simple, robust and well suited to measuring PWV and surface pressure, temperature and humidity in the convectively active remote mountain areas. Our instrumentation and initial findings described in Kursinski et al. (2008) are summarized below.

Monsoon Onset: The 2004 monsoon onset in Sonora, Mexico was evident as a large PWV increase that extended over several

continued on page 19

From Gochis, page 2: A view from the Golden Years of the North American Monsoon Experiment

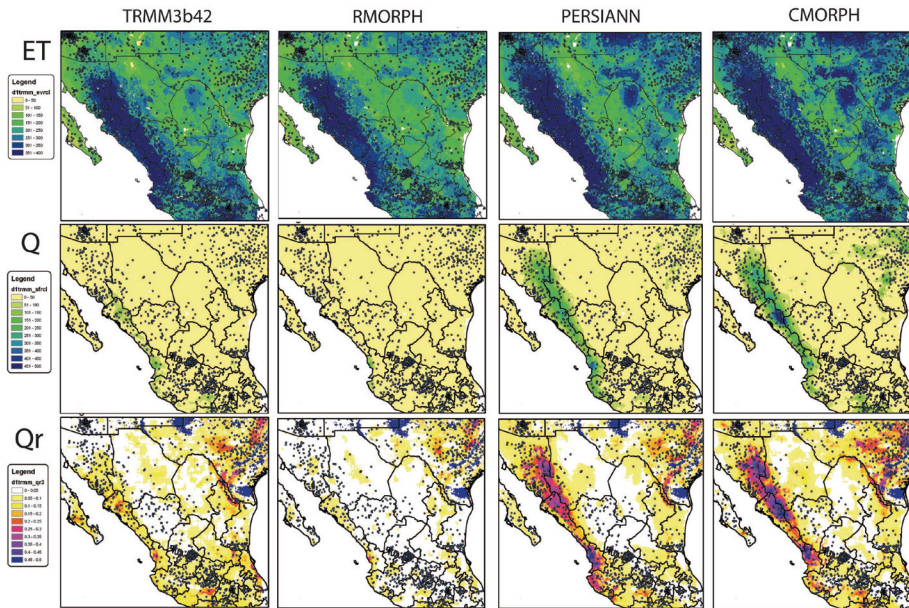


Figure 2: Jul-Aug 2004 Noah-HRLDAS simulated total evapotranspiration (ET, a-d), accumulated surface runoff (Q, e-h) and runoff fraction (Qr, i-l) from the RMORPH, TRMM3b42, CCMORPH and PERSIANN satellite QPE products. From Gochis et al., 2008.

From Gutzler et al., page 6: Atmospheric simulations of the 2004 North American Monsoon circulation: NAMAP2

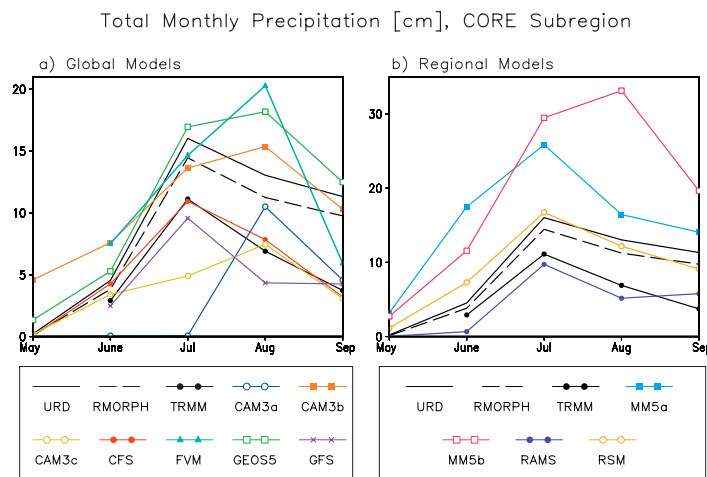
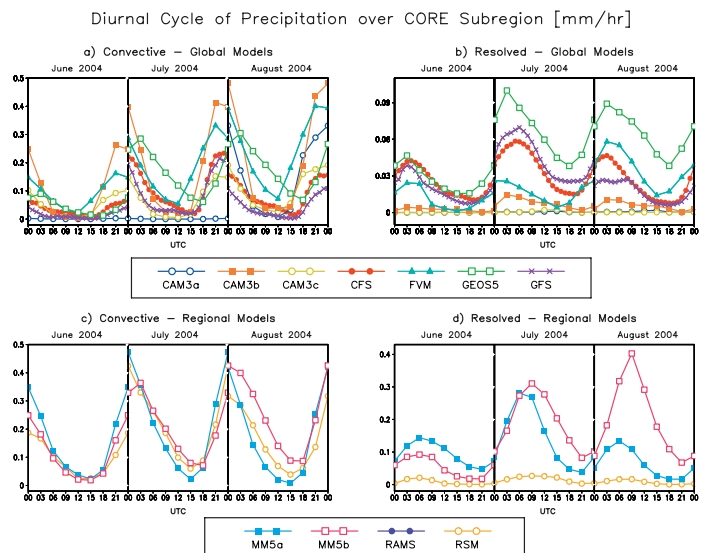


Figure 2: Time series of total monthly precipitation [cm] averaged over the CORE subregion, May-Sept 2004, simulated by (a) global models (b) regional models. Three estimates based on observations are shown as black lines in each plot.

Figure 3: Diurnal cycle of convective precipitation (left column, plots a and c) and resolved precipitation (right column, plots b and d), simulated by global models (a and b) and regional models (c and d) in the CORE subregion. The diurnal cycle was calculated as the monthly averaged hourly rain rate [mm/hr] in three-hour increments, for the months of June, July and August 2004. Time is shown as UTC. Note the much-expanded ordinate scale in plot (b).



From Higgins et al., page 9: Relationships between Gulf of California moisture surges and tropical cyclones in the Eastern Pacific Basin

From Rowe et al., page 12: Radar-based studies of convection in NAME

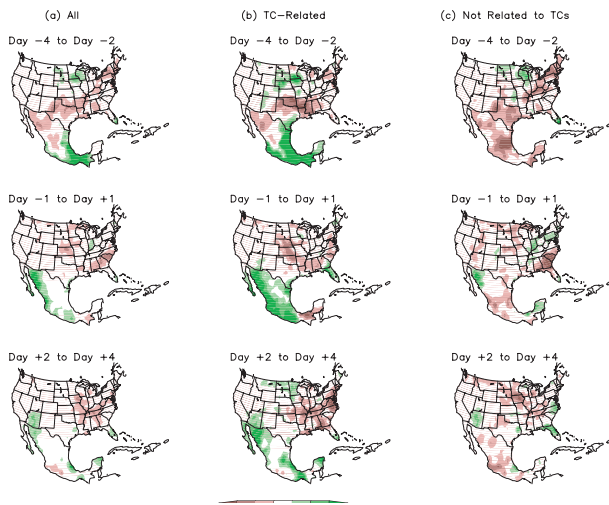


Figure 1. Composite evolution of accumulated precipitation anomalies (mm) for (a) all surges, (b) TC-related surges and (c) surges not related to TCs. Surges are keyed to Yuma, AZ. Day 0 is the onset date of the surges at Yuma. The accumulation period relative to onset is indicated on each panel. The shading interval is 1 mm day⁻¹ and values greater than 1 mm day⁻¹ (less than -1 mm day⁻¹) are shaded dark (light). The number of cases in each composite is given in Table 1, page 9.

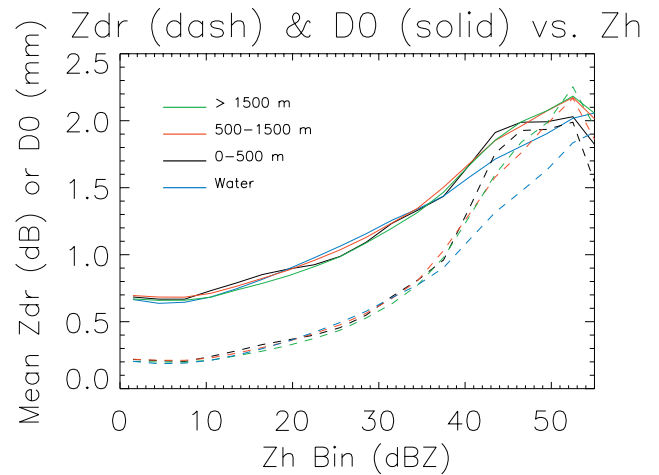


Figure 2. Near-surface differential reflectivity (ZDR) and median drop diameter (D0) as functions of reflectivity (ZH) for four terrain bands: over water, land 0-500 m, 500-1500 m, and 1500+ m MSL. Data from S-Pol during the NAME deployment (8 July-21 August 2004).

From Kursinski et al, Page 14: GPS observations of precipitable water and implications for the predictability of precipitation during the North American Monsoon

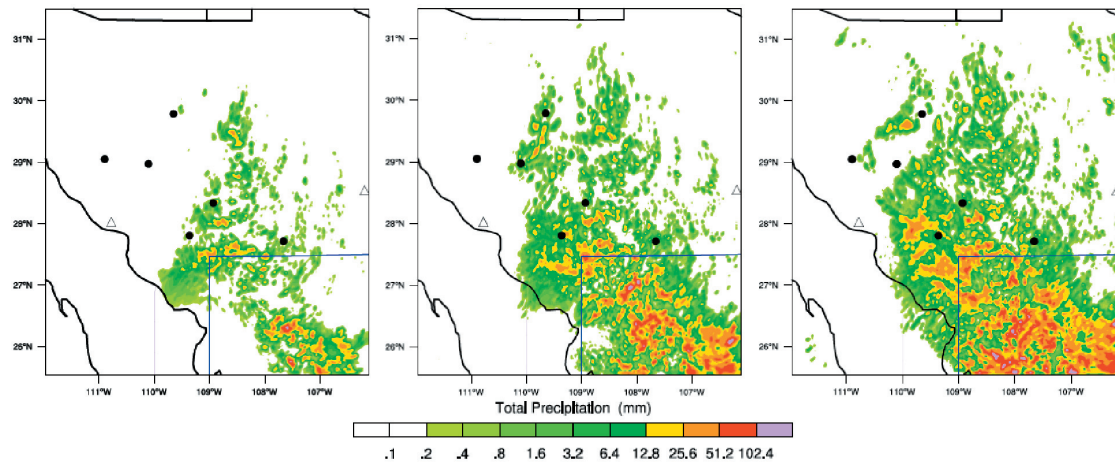


Figure 1. WRF simulations of accumulated precipitation for three different initial PWV fields, 95%, 100% and 105% of the ETA analysis PWV for July 29, 2004. Black dots indicate the locations of our GPS receivers. Triangles indicate the Empalme and Chihuahua radiosonde locations. Precipitation statistics in Figure 2 were derived in the southeastern region enclosed by the thin blue line.

From Vivoni et al, page 21: Relation between Surface Flux Measurements and Hydrologic Conditions in a subtropical scrubland during the North American Monsoon

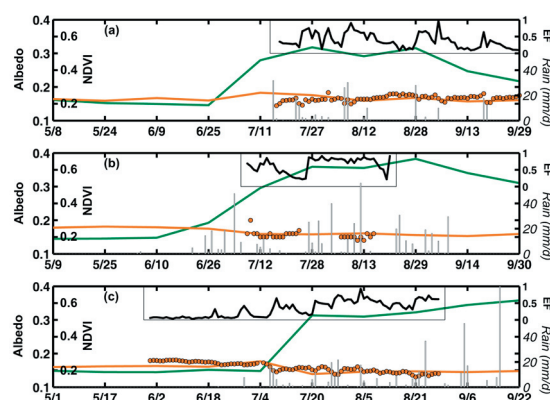


Figure 2. Seasonal evolution and interannual variability of rainfall, surface fluxes and land surface conditions at the EC tower for three monsoons: (a) 2004, (b) 2006, and (c) 2007. Rainfall (mm/day) is obtained from a tipping bucket rain gauge (gray bars). The MODIS sensor used to derive NDVI (green solid line) and albedo (orange solid line). MODIS albedo is compared to daily estimates at the EC tower obtained as the ratio of outgoing to incoming shortwave radiation ($a = R_{\text{out}}/R_{\text{in}}$, orange circles). Daily estimates of surface turbulent fluxes (sensible heat, H and latent heat, λE) are used to compute the evaporative fraction, $EF = \lambda E / (\lambda E + H)$, black solid line.

From Vivoni et al, page 21: Relation between Surface Flux Measurements and Hydrologic Conditions in a subtropical scrubland during the North American Monsoon

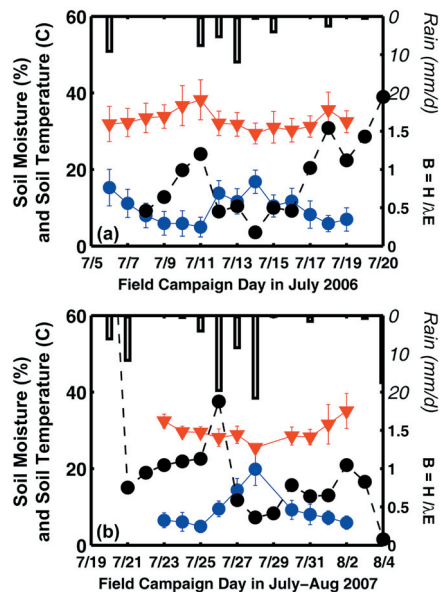


Figure 3. Footprint-averaged daily volumetric soil moisture (%), surface soil temperature (°C) and Bowen ratio ($B = H / \lambda E$, black circles) estimated from the EC tower for (a) 2006 and (b) 2007. Footprint-averaging considers all 30 plots in 250-m by 250-m pixel around tower (symbol is spatial average and bars represent ± 1 standard deviation). Daily rainfall (mm/day) from the tower site (bars) shown as reference.

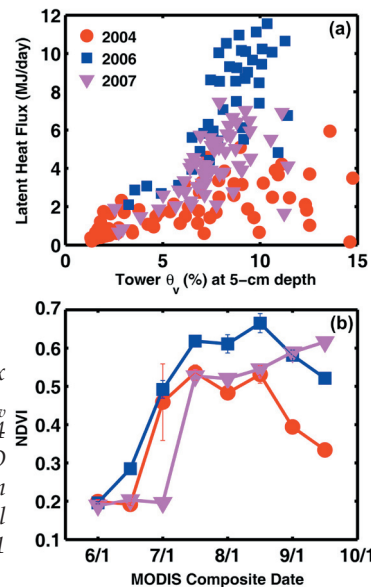


Figure 4. (a) Relation between daily latent heat flux (λE in MJ/day) and daily-average soil moisture (θ_v in %) obtained from a 5-cm depth sensor for 2004 (JD 205 to 275), 2006 (JD 189 to 228), and 2007 (JD 186 to 240). (b) Temporal evolution of NDVI from MODIS for 2004, 2006 and 2007, including spatial average of nine surrounding pixels (symbols) and ± 1 standard deviation (bars).

From Munoz-Arriola et al., page 24: Extended West-wide Seasonal Hydrological System: Seasonal Hydrological Prediction in the NAMS region

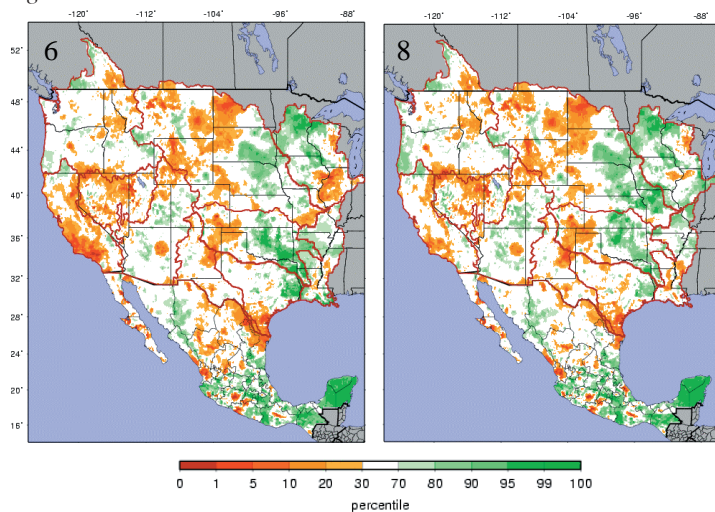
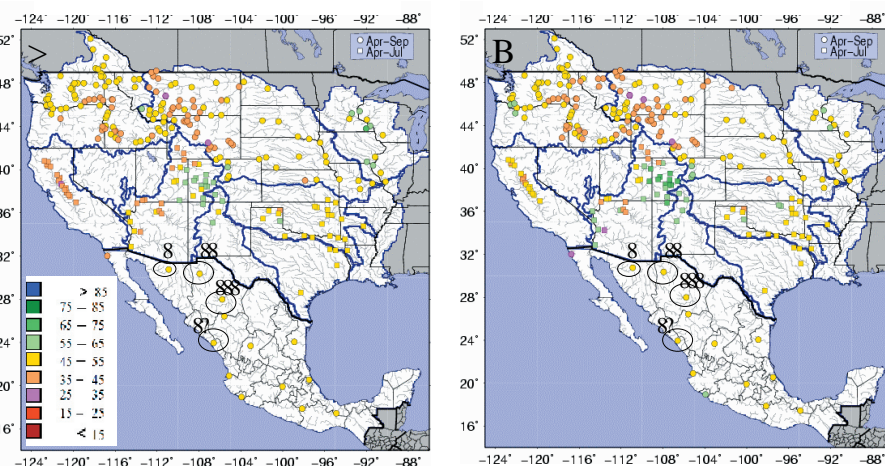


Figure 1. Soil Moisture Percentiles with respect to the 1960-1999 climatology for a) January 1st 2008 and b) January 15th 2008.

Figure 2. Forecasts effective 1/1/08 (a) and 1/15/08 (b) as streamflow percentiles for the western United States and Mexico for the period April-September (circles) and April-July (squares), 2008. Dots indicated percentiles relative to the 1960-1999 climatology. Circled points show locations of stations in the NAMS core region: I) Imuris, II) Casas Grandes, III) Conchos, and IV) Ixpalino.



continued from page 14

days beginning July 1. The water vapor-weighted winds derived from Empalme radiosonde profiles revealed that the rise in moisture during the monsoon onset and a preceding transitional wet period were associated with a shift in the winds from westerly to southerly and southeasterly.

Mid-August dynamical transition: The correlation between both precipitable water and surface specific humidity measured at Mazatan in the SMO foothills and at Hermosillo some 90 km to the west revealed a dynamical transition in mid-August from smaller, sub-synoptic scale structure to larger, synoptic-scale moisture structure. During the sub-synoptic phase in the SMO foothills, a positive feedback is indicated where near-daily precipitation supplied moisture maintains 15% higher surface mixing ratios that lower the lifting condensation level, facilitating initiation of moist convection.

Westward propagation of convection: Along the western edge of the SMO, precipitation typically occurs hours after the local temperature maximum, triggered by westward propagating convective disturbances. Observing the time-rate-of-change of PW, $dPWV/dt$, indicates that precipitation is typically preceded by a rapid increase in PWV associated with convergence of water vapor into the column and a sharp decrease in surface temperature associated with dense gust fronts created by evaporatively cooled downdrafts. As noted in other deep convective regimes, downdrafts are critical in storm organization, propagation and modulation of the daily temperature cycle.

III. Sensitivity of NAM precipitation to the initial water vapor field

The NAME PWV and surface condition measurements were utilized to assess the performance of the high resolution Weather Research and Forecasting (WRF) model. However, we discovered immediately that the discrepancies between our observations and WRF simulations were dominated by errors in the analyzed moisture field used to initialize WRF. We therefore focused on the sensitivity of convective precipitation in the WRF simulations to the initial PWV field in the NAM region.

A key ingredient in reproducing realistic behavior is model resolution. Summertime mid-latitude precipitation correlation scales east of the Rocky Mountains are generally much smaller than those in winter and smaller than the resolution of most GCMs (Kursinski and Mullen, 2008). Since 2003, we have used WRF to forecast NAM precipitation allowing us to experiment with and identify the configuration that produces the best overall simulations of NAM precipitation. We use 1.8 km resolution which is the resolution at which the accumulated convective precipitation became constant as resolution increases.

For the simulations presented here, we employed the WRF Model V2.2 with a 7.2 km grid outer domain and a 1.8 km grid inner domain and 37 vertical levels. NCEP's ETA 40 km model analysis was used to initialize the WRF simulations and provide periodic boundary conditions for the outer domain. The physics packages utilized are Lin cloud microphysics, RRTM longwave radiation, Goddard short wave radiation, Monin-Obukhov ETA surface-layer, Noah land-surface, and the Mellor-Yamada-Janjic TKE PBL scheme. In our experience in forecasting precipitation in the Southwest U.S., the Lin et al. microphysics scheme provides the best spatially distributed rainfall patterns, and more realistic amounts compared to other schemes. No convective parameterization was used as shallow and deep convection are resolved explicitly at this resolution.

For the preliminary precipitation sensitivity results presented here we chose two days, a medium precipitation day (July 29, 2004) and somewhat higher precipitation on the following day (July 30, 2004). To assess precipitation sensitivity to changes in

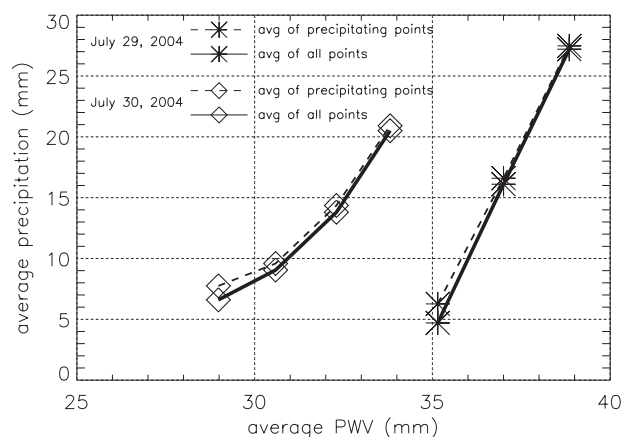


Figure 2. Average accumulated precipitation versus average initial PWV for July 29 and 30, 2004. Solid lines indicate averages over all grid points in the southeast region in Figure 1. Dashed lines indicate precipitation averaged over the subset of grid points in the southeast region experiencing precipitation.

PWV, we scaled the ETA analyzed precipitable water vapor field to 95%, 100% and 105% and used each to initialize a WRF model run. Cases were initialized at 5 a.m. local time when convective activity is generally minimal to avoid problems with the inability of ETA analysis resolution to capture the increasingly complex moisture field as convective activity increased during the day.

Figure 1 (page 16) shows the accumulated precipitation simulated by WRF for July 29, 2004 initialized by the ETA PWV field scaled to 95%, 100% and 105% of its nominal field. There is clearly a large overall increase in precipitation but the detailed response is complex. In fact, while most cells received more precipitation as PWV increased, precipitation in individual grid cells can either increase or decrease as PWV is increased. Extreme changes in precipitation at individual grid points as the initial PWV was increased by 5% ranged from 70 mm less precipitation to 90 mm more precipitation.

Figure 2 shows how accumulated precipitation averaged over the convectively active, southeastern region of the model domain (see Figure 1) increases as the early morning PWV increases. Precipitation sensitivities on both days are quite large. On July 29, 2004, average precipitation increases by 6 mm for every 1 mm of added average PWV. On July 30, precipitation increases more gradually with PWV. Interestingly, conditions on July 30 require about 5 mm or 15% less PWV to produce the same precipitation as on July 29.

IV. The accuracy of analyzed PWV

Now, to assess our ability to predict precipitation, we must determine the uncertainty in the initial water vapor field and contrast it with the sensitivity discussed in the previous section. To quantify the initial water vapor field error, we compared the NCEP North American Regional Reanalysis (NARR) PWV with the measured GPS PWV field. The NARR analyses are on a 32 km grid at 29 pressure levels, produced using the Eta 32km/45-layer model output every three hours.

For our comparisons of the NARR and GPS PWV estimates, we used the NARR grid point closest to each GPS location and coincident within 15 minutes. The results are summarized in Table 1. Figure 3 (page 20) shows the scatter of the NARR versus GPS PWV values at Mazatan, Sonora, Mexico, revealing both random and systematic discrepancies between the two data sets. The quadratic fit in the figure indicates the range of NARR PWV values is somewhat compressed on average relative to that measured by GPS. On average NARR produces 12 mm when

GPS measures 9 mm of PWV whereas when GPS measures 56 mm, NARR shows 50 mm. The scatter about the curve has a 1-sigma spread of about 5 mm which, given the 1.5 mm GPS PWV errors, is due primarily to the NARR procedures.

The standard deviation of the NARR PWV errors relative to GPS range from 11 to 18%. The smaller 7% discrepancy between the NARR and the Empalme radiosonde PWV is presumably because the Empalme data has been assimilated into the NARR. While the NARR water vapor errors are fairly good, the sensitivity described in the previous section suggests PWV errors of this magnitude lead to large errors in model precipitation. According to the sensitivity study, a 14% PWV error like that at Mazatan can overestimate the domain average precipitation by 15 to 30 mm.

V. Conclusions

Our results represent an initial quantification of a key issue regarding precipitation forecasting in the NAM region. The results are limited to only two days of simulations and have assessed sensitivity only to PWV. Still, our evaluations over the past four years indicate this model simulates precipitation behavior rather realistically in the NAM region but that the model sensitivity results must be considered seriously.

Our preliminary results indicate that when conditions are right to support moist convection and precipitation, the sensitivity of precipitation to small changes in the water vapor field is quite large within the high resolution WRF simulations. This sensitivity suggests that present knowledge of water vapor in the NAM region is inadequate to accurately forecast precipitation there.

We also found that the peak precipitation sensitivity for July 29 was about 40% higher than on July 30. The threshold PWV at which precipitation begins to occur is higher on July 29 as well. We speculate that this variation in sensitivity is associated with differences in large-scale forcing between the two days. On July 30, the mid-level northeasterly flow was very favorable for organized storms in the Mexican states of Sonora and Sinaloa to propagate from the high terrain into the coastal areas. As a result, the 95, 100 and 105% July 30 case storm organization exhibited similar overall structure despite differences in PWV. In general, the more important the large mesoscale to synoptic forcing, the less one would expect the modes of convection to be sensitive to small changes in PWV. In contrast, the 29 July case exhibited lighter mid and upper level winds over Sonora with less organization suggesting that varying PWV is more

Location	bias (mm)	Stdev (mm)	Fractional Stdev
Creel	1.22	2.5	13%
Yecora	0.95	3.5	11%
Moctezuma	-1.36	5.9	17.7%
Tesopaco	-1.32	4.9	11%
Mazatan	-0.59	5.4	13.5%
Hermosillo	3.14	5.3	11%
Empalme sonde	-1.86	3.4	7%

Table 1: NARR-GPS PWV statistics.

important to convective storm development when storms are less organized. We note that our simulations have so far only addressed sensitivity to PWV not the vertical variation in water vapor. Distributing the changes in PWV throughout the troposphere might lead to less entrainment of dry air resulting in more precipitation whereas adjusting the PWV only in lowest 100 mb, say, might have larger impacts on the intensity of convection and its rain production. Nevertheless, as an initial sensitivity study, very small changes in PWV are clearly important in model simulations of precipitation.

The most obvious implication of the sensitivity study presented here is that short-term warm season precipitation forecasts in the NAM region will be poor, particularly in Mexico, until the moisture analysis accuracy is improved significantly. This in turn requires that better moisture observations be made in the area which, given the limitations of satellite observations, will likely have to come from a combination of upward looking surface observations and more balloon measurements. An inexpensive network of GPS receivers at a subset of the precipitation gauge locations (Gochis et al., 2004) would dramatically improve the present data void in Mexico and measure interannual variability and long term trends. The same arguments may also be made for other deep convection regimes of the tropics where high temporal and spatial resolution data is entirely lacking.

In terms of predictive skill, the significantly better realism of the high resolution simulations presented here relative to poor performance of coarser resolution models (e.g., Lee et al., 2007) suggest that, at the moment, accurate representation of convective precipitation in the NAM area requires very fine model resolution to explicitly model convection accurately, resolution that will not appear in global climate models any time soon. Regional models imbedded in GCMs may succeed, but will be numerically intensive. Without such fine scale explicit modeling, the sensitivity we have identified will have to be captured via parameterizations derived from high resolution results, assuming such results can be verified. Although it is not clear if present observational sampling is sufficient, we will attempt to assess the realism of the WRF precipitation sensitivity using rain gauge (Gochis et al., 2004) and GPS PWV observations to determine the true precipitation sensitivity to variations in early morning PWV.

Acknowledgements

We thank Francina Dominguez for extracting the NARR data collocated with the GPS data. We also thank Jay Fein and NSF for funding the data acquisition via the Small Grant for Exploratory Research 0434790, after we were unable to secure funding from NOAA, and supporting some of this data analysis via grant 0551448. We also thank ONR for funding the computer cluster used to generate the simulations presented here. We thank Bob Maddox for many helpful comments

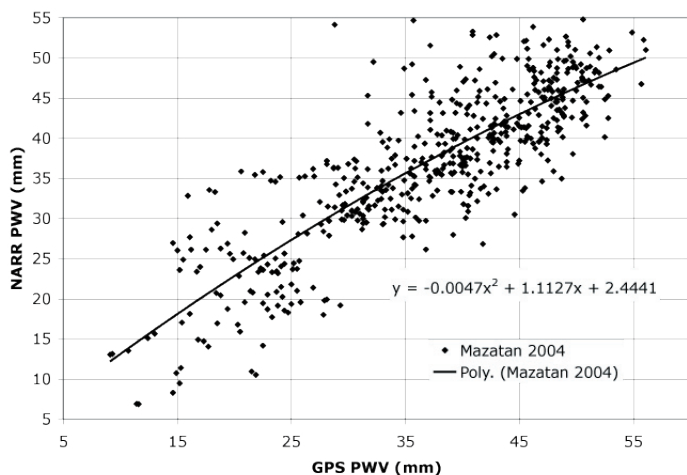


Figure 3: Comparison of GPS and NARR PWV at Mazatan in Sonora, Mexico.

regarding this research and this manuscript.

References

- Adams, D. K. and A. Comrie, 1997: The North American Monsoon. *Bull. Amer. Meteor. Soc.*, **78**, 2197-2213.
- Gochis, D.J., A. Jimenez, C.J. Watts, W.J. Shuttleworth, J. Garatuza-Payan, 2004: Analysis of 2002 and 2003 warm-season precipitation from the North American Monsoon Experiment event rain gauge network. *Mon. Wea. Review*, **132**, 2938-2953.
- Higgins, R.W. D. Ahijevych, J. Amador, A. Barros, E.H. Berbery, E. Caetano, R. Carbone, P. Ciesielski, R. Cifelli, M. Cortez-Vazquez, A. Douglas, M. Douglas, G. Emmanuel, C. Fairall, D. Gochis, D. Gutzler, T. Jackson, R. Johnson, C. King, T. Lang, M.I. Lee, D. Lettenmaier, R. Lobato, V. Magaña, J. Meiten, K. Mo, S. Nesbitt, F. Ocampo-Torres, E. Pytlak, P. Rogers, S. Rutledge, J. Schemm, S. Schubert, A. White, C. Williams, A. Wood, R. Zamora, and C. Zhang, 2006: The North American Monsoon Experiment (NAME) 2004 field campaign and modeling strategy. *Bull. Amer. Meteor. Soc.*, **87**(1), 79-94.
- Kursinski, A. L., and S. L. Mullen, 2008: Spatiotemporal variability of hourly precipitation over the Eastern Contiguous United States from Stage IV multisensor analyses, *Journal of Hydrometeorology*, **9**, 3-21.
- Kursinski, E.R., R. A. Bennett, D. Gochis, S. I. Gutman, K. L. Holub, R. Mastaler, C. Minjarez Sosa, I. Minjarez Sosa, and T. van Hove, 2008: Water vapor and surface observations in northwestern Mexico during the 2004 NAME Enhanced Observing Period, *Geophys. Res. Lett.*, **35**.
- Lee, M.I., S.D. Schubert, M.J. Suarez, I.M. Held, A. Kumar, T.L. Bell, J.K.E. Schemm, N.C. Lau, J.J. Ploshay, H.K. Kim, and S.H. Yoo, 2007: Sensitivity to horizontal resolution in the AGCM simulations of warm season diurnal cycle of Precipitation over the United States and Northern Mexico. *J. Climate*, **20**, 1862-1881.
- Weckwerth T. M., D. B. Parsons, S. E. Koch, J. A. Moore, M. A. Lemone, B. B. Demoz, C. Flamant, B. Geerts, J. Wang, and W. F. Feltz, 2004: An overview of the international H2O project (IHOP 2002) and some preliminary highlights, *Bull. Amer. Meteor. Soc.*, **85**, 253-277 DOI: 10.1175/BAMS-85-2-253.

Relation between surface flux measurements and hydrologic conditions in a subtropical scrubland during the North American Monsoon

Vivoni, E.R.¹, C.J. Watts², J.C. Rodríguez², J. Garatuza-Payan³, L.A. Méndez-Barroso¹, E.A. Yopez⁴, J. Saiz-Hernández², and D.J. Gochis⁵
¹Department of Earth and Environmental Science, New Mexico Institute of Mining and Technology, ²Departamento de Física, Universidad de Sonora, México. ³Departamento de Ciencias del Agua y del Medioambiente, Instituto Tecnológico de Sonora, México. ⁴Department of Biology, University of New Mexico, ⁵. National Center for Atmospheric Research, USA.
 Corresponding author: vivoni@nmt.edu.

Introduction

The North American monsoon (NAM) is the primary climatological phenomenon in the southwestern United States and northwestern Mexico, leading to large changes in precipitation, atmospheric conditions, vegetation and overall land surface properties (e.g., Douglas et al., 1993). Previous studies carried out by the North American Monsoon Experiment (NAME) have focused on the relationship and potential feedbacks between the NAM and the conditions of the land surface, including changes in vegetation, soil moisture and streamflow (Zhu et al., 2005; Gochis et al., 2006; Watts et al., 2007; Vivoni et al., 2007). Evidence from these studies suggests dramatic transitions in the hydrological conditions of the region. For example, in the seasonal march of the runoff ratio (Gochis et al., 2006) and in sharp changes in the surface fluxes (Watts et al., 2007). Here, we present multiple-year evidence for the relation between surface flux measurements and hydrologic conditions in a subtropical scrubland, one of the major regional ecosystems, which experiences significant greening during the NAM (Salinas-Zavala et al., 2002; Watts et al., 2007). The analysis is based on measurements at and around an Eddy Covariance (EC) tower located in Rayón, Sonora, Mexico within the Río San Miguel river (~3500 km²) basin.

Surface Flux Measurements

Recent land-atmosphere interaction studies in the NAM region have focused on understanding the impact of vegetation greening on the measurement of soil moisture and energy balance components, including evapotranspiration. While these efforts began during the NAME 2004 campaign, subsequent studies have been sponsored by NSF, CONACYT and NOAA. Our focus is on the relation of surface fluxes, soil moisture and land surface conditions at the Rayón EC site (denoted as STS in Watts et al., 2007). The site is located at ~630 m in the Río San Miguel, a large ephemeral river basin, flowing north to south in the northern Sierra Madre Occidental. Vegetation at the site is classified as subtropical scrubland and is a mixture of trees, shrubs and desert cactus that respond to the precipitation pulses

during the NAM. Soil profiles in the region are shallow (~70 cm in depth above an impermeable clay lens) and primarily composed of loamy sand and sandy loam with intermixed clasts.

Figure 1a (page 22) illustrates the experimental design for surface fluxes and footprint measurements of soil moisture and temperature. The footprint of the EC tower is defined here as a 250-m by 250-m region around the site, selected based on the pixel dimensions of the MODIS sensor. Within the EC tower footprint (see below), 30 sampling plots were established to relate these land surface conditions to the surface flux measurements. The 9-m tower contains a 3D sonic anemometer, as well as high frequency measurements of air temperature and relative humidity to estimate the covariance terms necessary to obtain the latent and sensible heat fluxes (Watts et al., 2007). Hydrometeorological observations at the site also include precipitation, soil moisture and temperature (at three depths), and radiation components used to estimate albedo and net radiation. Operation of the Rayón EC site has concentrated on summer campaign periods in 2004, 2006 and 2007, in particular to capture the changing conditions during the NAM onset, peak and demise (e.g. vegetation greening, see Figure 1b, c).

In Figure 2 (page 16), we present a comparison of remotely-sensed and field observations of rainfall, surface fluxes and land surface conditions during three monsoon periods (2004, 2006, 2007) at the EC tower site. Several interesting transitions are observed in vegetation cover, surface albedo and surface fluxes during the NAM, as well as important differences among the monsoon seasons. Vegetation dynamics are captured by the Normalized Difference Vegetation Index (NDVI) estimated at the tower pixel (250-m by 250-m) from 16-day MODIS composites. Vegetation dynamics are clearly tied to the daily precipitation, with early or late monsoon greening tightly related to the onset of precipitation. Similarly, the decrease in NDVI during the monsoon demise is tied to the available precipitation in the late summer. It is interesting to compare,

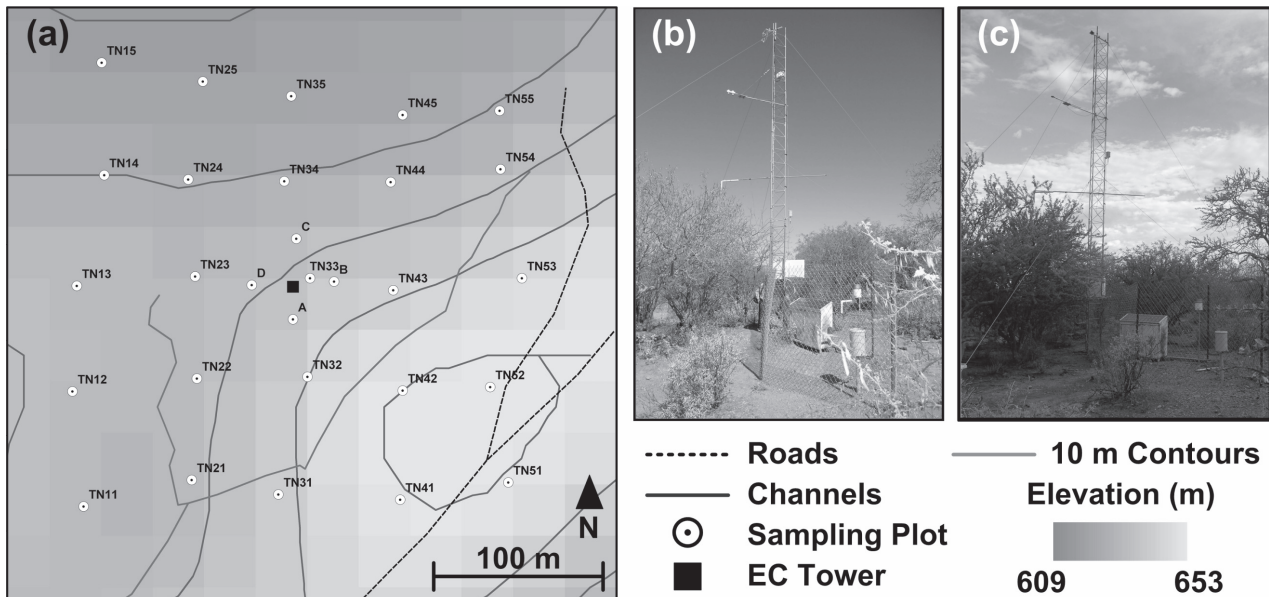


Figure 1. EC tower location and footprint sampling plots in Rayón, Sonora (30.04°N, 110.67°W). (a) Thirty sampling plots (white circles) in a 250-m box surrounding tower site (black square) overlain on a 30-m DEM (Digital Elevation Model) derived from ASTER (Advanced Spaceborne Thermal Emission and Reflection Radiometer). Roads and channels were traced using a GPS. (b) and (c) are photographs of the EC tower taken during a June period prior to the monsoon onset and a July period after monsoon greening, respectively.

for example, monsoon 2006 (Figure 2b) with a high peak *NDVI* and early onset, with monsoon 2007 (Figure 2c), which showed a reduced *NDVI* peak, a later onset but longer duration.

Vegetation greening is closely tied to the changes in albedo observed at the site from two sources: MODIS 16-day broadband albedo composites (1-km resolution) and EC tower albedo estimates. Comparison between the two albedo estimates is remarkably good, given the differences in spatial resolution (1 km² versus ~4 m² field of view), suggesting a spatially coherent change in vegetation cover in the vicinity of the tower. The clearest transition in albedo is observed for monsoon 2007 (Figure 2c) which spans the largest time period. Note that the vegetation greening indicated by increasing *NDVI* is coincident with the decrease in albedo. As expected, the land surface greening decreases the surface albedo, although the change is not very large (from ~0.18 to ~0.15), possibly due to the low leaf area and the extensive bare ground in this ecosystem. Given the high amounts of incoming solar radiation at the site, however, even small changes in albedo can significantly affect the radiation balance. Note that as vegetation cover is reduced in the late monsoon 2004 (Figure 2a), the albedo of the land surface begins to increase once again to reflect the drier, desert conditions.

Along with changes in albedo, vegetation greening leads to significant variations in the partitioning of surface turbulent fluxes, as captured by the evaporative fraction, $EF = \lambda E / (\lambda E + H)$, where H and λE are the daily-averaged sensible and latent heat fluxes. This is most clearly observed in monsoon 2007 (Figure 2c) where the measurements span the monsoon onset and vegetation response. Note the low values of EF (near zero), implying higher sensible heat fluxes, prior to the *NDVI* increase, and the dramatic increase in EF (~0.7 to 0.9) as available soil moisture from precipitation pulses is transferred back to the atmosphere via evapotranspiration. During each summer, individual storm events lead to increases in EF (e.g., higher latent heat flux) that are sustained over periods of several days. Interestingly, for periods with consecutive storms (low interstorm duration), sustained EF at high values may last for several weeks, for example in monsoon 2006 (Figure 2c). During the monsoon demise, vegetation becomes senescent and the

EF decreases toward low values (see latter part of monsoon 2004, Figure 2a), implying a return to high sensible heat fluxes at the land surface.

Footprint-Averaged Hydrologic Conditions

In an effort to understand land-atmosphere interactions, we conducted a set of intensive surface measurements in the tower footprint (Figure 1a). For simplicity, we defined the footprint as 250-m by 250-m box around the tower, while recognizing that the actual measurement footprint will vary with wind conditions. For our purposes, this definition allows comparison of the estimated surface conditions to remotely-sensed observations from MODIS. As shown in Figure 1a, the topographic conditions around the tower are fairly uniform, as determined from a satellite-derived digital elevation model. Nevertheless, terrain variability at the site does include two stream channels, which have more abundant riparian vegetation as compared to exposed hillslopes at the site. As a result, we expected to capture spatiotemporal variations in soil temperature and moisture through daily sampling at the thirty (30) sampling plots in the tower footprint. Each sampling plot (~1m by 1m) was sampled at similar times each day during two week intervals in July and August 2006 and 2007. Measurements were performed using portable sensors, as described more fully in Vivoni et al. (2007).

Figure 3 (page 17) presents a comparison between the footprint-averaged, daily soil moisture (blue circles) and temperature (red triangles) conditions and the estimated daily Bowen Ratio ($B = H/\lambda E$, black circles). Surface fluxes and footprint hydrologic conditions are presented for monsoon 2006 (July 5 to 20, Figure 3a) and monsoon 2007 (July 19 to August 4, Figure 3b). The soil moisture and temperature symbols represent the average of the 30 plots, while the bars capture the spatial variability as ± 1 std. The daily precipitation (bars) is included for reference. Note the good correspondence between the soil moisture and soil temperature and their relation to storm and interstorm periods. As expected, precipitation pulses promote a decrease in soil temperature and an increase in soil moisture, with consecutive storms leading to sustained wet and cool surface conditions. Interestingly, the spatial variability in the footprint is different in the two years, with monsoon 2007 exhibiting smaller spatial

variations in soil moisture and temperature, due to the effects of sustained cloud cover on limiting incoming solar radiation.

Of particular relevance is the relation between land surface conditions and the Bowen Ratio measured during monsoons 2006 and 2007. Note the excellent correspondence between footprint-averaged soil moisture and B , where periods of high B (large H) occur during interstorm periods, with rapid decreases in B (high λE) after precipitation pulses wet the land surface. Further analysis of the relation between B and footprint-averaged soil moisture (not shown) indicates that a power law behavior is observed for both monsoon seasons: $B = 4.95 <\theta>^{-0.95}$ ($R^2 = 0.6$), where $<\theta>$ is the footprint-averaged, daily soil moisture (%). This relation is significantly weakened when using the soil moisture conditions at the sampling plot near the tower. This suggests that the surface flux measurements are directly linked to the averaged soil moisture conditions in the tower footprint. Analysis comparing the tower and footprint-averaged conditions also revealed that the region around the tower is wetter and cooler than the tower plot, on average, for the two sampling periods.

Soil Moisture Controls on Evapotranspiration

The relation between surface fluxes and soil moisture conditions is particularly important as it forms an important parameterization in many land surface models (e.g. Vivoni et al., 2005). Typically, actual evapotranspiration (ET) is regulated by the amount of soil moisture present in the root zone, following a functional form that recognizes soil moisture limitations on ET below a threshold value (Rodríguez-Iturbe and Porporato, 2004). The functional form varies across different land surface models, but is generally assumed to be constant in time, with appropriate parameters selected for the ecosystem of interest. Unfortunately, few studies have attempted to establish the appropriate relationships between ET and soil moisture in ecosystems experiencing monsoonal greening and pulsed precipitation. As a result, most hydrological and climate models operating in the NAM region do not adequately capture vegetation dynamics in the parameterization of surface fluxes.

Figure 4 (Page 17) provides initial evidence for the temporal (and vegetation-dependent) variation of the relation between ET and soil moisture in the subtropical scrubland. Daily estimates of latent heat flux (λE), consisting of both evaporation and transpiration, are plotted as a function of the daily-averaged soil moisture from the tower sensor (at 5-cm depth, θ in vol. %) in Figure 4a. We use the tower site data due to the longer period of coincident measurements. Note the differences in the relation between λE and θ for each monsoon, suggesting the functional form may have interannual variations that depend on the vegetation state. For example, monsoon 2004 exhibits a maximum λE that asymptotes for high soil moisture values (~12 to 15 %) at ~4 MJ/day, while monsoon 2006 shows a maximum λE of nearly 12 MJ/day for soil moisture values of 10 to 12%.

Inspection of the $NDVI$ time series for each monsoon season (Figure 4b), indicates that the sequence of $\lambda E(\theta)$ relations follows a similar order to that observed in the maximum $NDVI$. Monsoon 2006, which exhibited the higher values of λE for a given θ , also shows the highest vegetation greenness. This suggests that the subtropical scrubland at the EC tower site has a greater transpiration capacity during years with increased biomass resulting from above-average precipitation. As a result, the soil moisture control on ET varies temporally according to the ecosystem state.

Discussion and Conclusions

The evidence presented here on the interactions of surface fluxes

and hydrological conditions in the North American monsoon region is based upon integrated, multiple-year studies at an eddy covariance tower site in the subtropical scrubland of northern Sonora, Mexico. The use of remote sensing data, EC tower observations and footprint measurements of surface conditions have revealed that: (1) the onset of the NAM leads to dramatic changes in surface properties and the partitioning of energy fluxes; (2) footprint-averaged soil moisture and temperature conditions are closely related to the surface fluxes; and (3) considerable variations exist between monsoon seasons, leading to vegetation-dependence on the relation between soil moisture and ET . On-going and future efforts in the study region include a detailed ET partitioning experiment based on the isotopic signature of water vapor, vegetation and soil samples (summer 2007); installation of a new EC tower site in the Río San Miguel (summer 2008); and land surface modeling using one-dimensional and distributed approaches to assess implications of our findings toward simulations and forecasts in the NAM region.

References

- Douglas, M. W., Maddox, R. A., Howard, K., and S. Reyes, 1993: The Mexican monsoon. *J. Climate*, **6**, 1665-1677.
- Gochis, D. J., Brito-Castillo, L., and W. J. Shuttleworth, 2006: Hydroclimatology of the North American monsoon region in northwest Mexico. *J. Hydrol.*, **316**, 1-4, 53-70.
- Rodríguez-Iturbe, I., and A. Porporato, 2004: Ecohydrology of water-controlled ecosystems: Soil moisture and plant dynamics. Cambridge University Press, 442 pp.
- Salinas-Zavala, C. A., Douglas, A. V., and H. F. Díaz, 2002: Interannual variability of $NDVI$ in northwest Mexico. Associated climatic mechanisms and ecological implications. *Remote Sens. Env.*, **82**, 2-3, 417-430.
- Vivoni, E. R., Ivanov, V. Y., Bras, R. L., and D. Entekhabi, 2005: On the effects of triangulated terrain resolution on distributed hydrologic model response. *Hydrol. Process.*, **19**(11): 2101-2122.
- Vivoni, E. R., Gutiérrez-Jurado, H. A., Aragón, C.A., Méndez-Barroso, L. A., Rinehart, A. J., Wyckoff, R. L., Rodríguez, J. C., Watts, C. J., Bolten, J. D., Lakshmi, V. and Jackson, T. J. 2007: Variation of hydrometeorological conditions along a topographic transect in northwestern Mexico during the North American monsoon. *J. Climate*, **20**(9), 1792-1809.
- Watts, C. J., Scott, R. L., Garatuza-Payan, J., Rodríguez, J. C., Prueger, J. H., Kustas, W. P. and Douglas, M. 2007: Changes in vegetation condition and surface fluxes during NAME 2004. *J. Climate*, **20**(9), 1810-1820.
- Zhu, C., Lettenmaier, D. P., and T. Cavazos, 2005: Role of antecedent land surface conditions on North American monsoon rainfall variability. *J. Climate*, **18**, 3104-3121.

Extended west-wide seasonal hydrological system: Seasonal hydrological prediction in the NAMS regions

Munoz-Arriola, F¹, D.P. Lettenmaier¹, C. Zhu¹, A.W. Wood¹, R. Lobato Sánchez², and A. Wagner Gomes²

¹Department of Civil and Environmental Engineering, University of Washington, Seattle, USA., ²Coordinación de Hidrología Instituto Mexicano de Tecnología del Agua, Morelos, México.

Corresponding author: dennisl@u.washington.edu

1. Introduction

Hydrologic forecasting in areas constrained by the availability of hydrometeorological records is a major challenge in water resources management. The University of Washington West-wide Seasonal Hydrologic Forecast system (WWHFS, Wood and Lettenmaier, 2006; www.hydro.washington.edu/forecast/westwide), which generates nowcasts of soil moisture and runoff updated daily in near-real time for the western U.S., has recently been extended into Mexico (see also the Daily West-daily Monitor; <http://www.hydro.washington.edu/forecast/westwide/spatial/ncast/index.shtml>). In addition to the nowcasts (see Figure 1, page 17), the WWHFS produces seasonal streamflow forecasts with monthly updates (biweekly in winter) at almost 250 forecast points in the western U.S., to which we have added 14 forecast points in Mexico (see Figure 2 page 17). The forecast points in Mexico are mostly small river basins which serve as index locations (minimal water management effects upstream) that are characterized by relatively low natural streamflow as compared with the western U.S. sites. Included among the 14 forecast points in Mexico are four points located in the North American Monsoon System (NAMS) region (circled in Figure 2). All of these points are within river basins where streamflow downstream of the forecast points is intensively used for irrigation, and where improved streamflow forecast accuracy could have significant economic benefits.

In addition to the western U.S. and Mexico forecasts now being produced by the WWHFS, a similar system at Princeton University (<http://hydrology.princeton.edu/~luo/research/FORECAST/current.php>) produces streamflow forecasts over the Eastern U.S., and we are in the process of merging these two systems. The merged U.S. system, combined with expansion into Mexico, will produce a seamless streamflow forecast system over all of the U.S. and Mexico. The inclusion of Mexico within the expanded domain nonetheless presents certain challenges. Climate and hydrological information over Mexico is sparser than over much of the U.S., and, in contrast to the western U.S. where most WWHFS forecast points are now located, there is little snow water storage, and hydrologic forecast skill is governed primarily by knowledge (or lack) of soil moisture on the forecast date.

2. Methodology

The WWHFS nowcast system utilizes station data provided by the Applied Climate Information System (ACIS) over the continental U.S., and by Servicio Meteorológico Nacional (SMN) over Mexico (with a "fallback" option that uses NCEP weather forecast model nowcast fields (NDAS) when the real-time station data are not available). Station data from both sources are gridded to the 1/8 degree North American Land Data Assimilation System (N-LDAS) grid, and over the western U.S., are adjusted for orographic effects using the PRISM (Precipitation Regression on Independent Slopes Method) approach. No PRISM adjustments are feasible over Mexico at present.

Seasonal forecasts currently are based on the National Weather Service Ensemble Streamflow Prediction method (ESP; essentially resampling of climatology), with a method of downscaling driven by NCEP Climate Forecast System (CFS) forecasts to be added soon. These in turn are being used to force

the Variable Infiltration Capacity (VIC) macroscale hydrology model, initialized with nowcast soil moisture and snow water storage, to produce streamflow ensembles. One-year lead time streamflow forecasts updated monthly (twice monthly in winter) are now being produced at the 14 streamflow forecast points in Mexico, in addition to the western U.S. forecast points as shown in Figure 2.

In the WWHFS, nowcasts are produced using gridded forcing data derived from real-time station data as described above to force the VIC model up to the time of forecast, thus producing the nowcasts (which are updated on a daily basis). VIC requires precipitation, and surface air temperature as model forcings, which are taken directly from gridded data. Other surface forcing variables, including surface humidity, and downward solar and longwave radiation, are derived from daily minimum or average temperature, whereas surface wind is taken from the NCEP North American Regional Reanalysis (NARR, available to within two days of present) and NDAS thereafter.

Forty streamflow ensemble members are used in the ESP method to produce forecasts at each streamflow forecast point (within the U.S., we also use a synthetic ensemble method, described in Wood and Lettenmaier (2006), based on CPC "official" forecasts, however, these forecasts are not available over Mexico). The 40 ESP ensemble members are taken from the gridded climatological data for the period 1960 to 1999. VIC streamflow forecasts are post-processed (as percentiles and fractions of the long-term means) and are provided both in graphical and numerical formats available on the web.

The forecast points within Mexico were calibrated by Zhu and Lettenmaier (2007) and encompass different hydroclimatic regions, and water management considerations. We focus here on the four basins located within the NAMS region (Imuris, Ixpalino, Casas Grandes, and Conchos, shown in Figure 2). Imuris and Ixpalino are located in the western side of Sierra Madre Occidental and are sub basins of the Rio Sonora and Rio Ixpalino, respectively. Casas Grandes and Conchos are located in the eastern side of the Sierra Madre Occidental and are both within the Rio Bravo basin (Rio Grande). Streamflow at these stations is frequently affected by multiyear drought events, which have substantially impacted the region's agriculture in the past.

3. Results

Figure 1 shows the initial conditions used for the forecast system to produce the ESP simulations as percentiles of soil moisture with respect to the 1960-1999 climatology for January 1 and January 15, 2008. Soil moisture nowcasts are strongly influenced by antecedent precipitation, and hence influence the hydrologic forecasts. Figure 2 shows the ensemble mean summer 2008 forecast streamflow as percentiles of the 1971-2000 climatology made from the initial conditions for the 1st and the 15th of January of 2008. Different colours represent the percentiles of the forecast streamflow at each point, and the shapes of the points show the periods April-September and April-July (circles and squares, respectively). Initial conditions such as soil moisture obtained by the nowcast system show a strong effect on the seasonal hydrologic forecast. For example, over portions of California, where precipitation occurred on the 4th, 5th, and 9th of January with values exceeding 64 mm/day in some mountainous locations, a reduction in the area covered

by soil moisture percentiles below 50 is found (see Figure 1). These events are reflected in changes in the January 15, as compared with January 1 forecasts (Figure 2), in particular in the increment of the forecast April-July streamflow, which in some cases show ensemble means changing from the 35-45 to 45-55 percentile intervals. In Colorado, mountain precipitation events during the first and second weeks of January affected about one-third of the forecast points in the upper Colorado River basin, increasing the forecast April-July percentiles from the 45-55 to the 55-65 range. Some points in the upper Mississippi showed a decrease in the forecast summer streamflow between January 1 and 15, which was determined by the spread of low-percentile soil moisture areas in the basin. In contrast, the streamflow forecasts for points in Mexico showed little change between the January 1 and 15 forecasts – most likely because April-July forecasts for most of the forecast points in Mexico are dominated by monsoon precipitation, and are much less affected by winter initial conditions than are forecast points in the western U.S. Even for the Boquilla station though, located near the U.S. border between Baja California and California (outside the NAM domain), precipitation that occurred between the 5 and the 8 of January did not affect the streamflow forecasts as much as for the forecast points in California. This could be due, in part, to the lack of hydrometric stations in the basin. For those stations (Imuris, Ixpalino, Conchos, and Casas Grandes) that are located in the NAM domain, the forecasts are close

to the climatological mean during the monsoon season 2008, mostly because the persistence of soil moisture anomalies in the region is not sufficient to propagate an influence of wet initial conditions during the winter to the beginning of the monsoon season (see Zhu et al., 2007).

In general, the ESP method tends toward climatology as the forecast horizon increases. Streamflow in the NAMS-affected portion of Mexico is critical for agricultural production, and more accurate streamflow forecasts would be of great benefit to water resources management. In places such as Northwestern Mexico, winter and spring water surplus in dams determines the agricultural activities, while monsoon water resources are concentrated on storage.

4. References

- Wood, A.W. and D.P. Lettenmaier, 2006. A testbed for new seasonal hydrologic forecasting approaches in the western U.S., *Bulletin of the American Meteorological Society*, **87**(12), 1699-1712, doi:10.1175/BAMS-87-12-1699.
- Zhu C.M. and D.P. Lettenmaier, 2007. Long-term climate and derived surface hydrology and energy flux data for Mexico, 1925-2004, *Journal of Climate*, **20**, 1936-1946.
- Zhu C.M., T. Cavazos, and D.P. Lettenmaier, 2007. Role of Antecedent Land Surface Conditions in Warm Season Precipitation over Northwestern Mexico, *Journal of Climate*, **20**, 1774-1791.

The QUEST Working Group on Dust and the future of dust-cycle research

Durant, A.², S. P. Harrison¹, B. Maher³, Y. Balkanski⁴

¹School of Geographical Sciences / Dept. of Earth Sciences, University of Bristol, UK., ²School of Geographical Sciences, University of Bristol, UK., ³Lancaster Environment Centre, University of Lancaster, UK., ⁴Laboratoire des Sciences du Climat et l'Environnement/Institut Pierre-Simon, Paris, France

Corresponding author: adam.durant@bristol.ac.uk

Atmospheric dust both absorbs and scatters solar radiation (the direct radiative effect, RE), which alters the energy balance of the atmosphere. In addition, dust plays an important role in cloud microphysics, and impacts the formation and lifetime of clouds (the indirect RE), which influences the planetary albedo. According to the IPCC Fourth Assessment Report (Forster et al., 2007, pp. 167-168), state-of-the-art dust cycle modelling estimates of net top of the atmosphere (TOA) direct radiative forcing by dust range between -0.56 to +0.1 Wm⁻². Thus, there remains considerable uncertainty in both the sign and the magnitude of dust direct radiative forcing.

The overall magnitude of the direct and indirect radiative effect is determined by the amount of dust present in the atmosphere and the physical characteristics of dust particles. Dust emission estimates, including location, duration, and vertical flux of emitted dust, require high temporal and spatial resolution observations over an extended observation period. Satellite remote sensing provides a valuable tool for addressing these issues, but has relatively limited temporal coverage, and time-series measurements from key locations provide longer records but may not sample the spatial variability of dust loading adequately; there are relatively few studies that have attempted to address, in necessary detail, global dust emission and atmospheric loading. Consequently, estimates of the total global dust burden vary by over a factor of 2. Furthermore, dust cycle models still employ relatively simple representations of dust particle characteristics, with the largest uncertainties resulting from: poor description of (1) dust composition, related to the natural variability in dust mineralogy and inadequate knowledge of refractive indices, (2) particle shape, specifically the assumption in most dust-cycle models that dust particles are spherical, (3) the size distribution of transported dust particles, related to poor specification of dust-source particle

size distributions, and (4) the vertical distribution and amount of dust in the atmosphere. The absorptivity of dust particles remains one of the greatest uncertainties associated with the impact of dust on climate. Recent remote-sensing measurements indicate that dust is a poor absorber and effectively attenuates solar radiation. However, the standard shortwave refractive index commonly used in modelling the radiative effects of dust is derived from laboratory experiments carried out in the 1970s and early 1980s, and results in greater absorption of solar radiation than is implied by the remote-sensing data. Consequently, the TOA globally-averaged direct forcing from dust may be shifted to a net positive value in modelling studies that have utilised the older laboratory-derived refractive indices, whereas more recent studies based on remote sensing retrievals of dust refractive index suggest that the net forcing is dominantly negative (Figure 1, page 18).

The location and characterisation of dust sources is another weakness in state-of-the-art dust-cycle models. Many models treat palaeolake basins or low-lying areas more generally as preferential dust sources. Remote-sensing studies and field-based geomorphic mapping show that dust is emitted from a wide variety of different geomorphic settings, including e.g. inter-dunal depressions, the marginal areas of lakes and fluvial/alluvial fans. Dust sources are highly localised, with considerable temporal variability in emissions from specific sources. Furthermore, discrete sources within a region can be active at different times through the year. Incorporating this complexity in a modelling framework is challenging. The characterisation of sources in terms of dust physical and chemical properties poses another challenge: most modelling groups specify dust size distribution characteristics based on global soil data sets which provide "average" properties over large areas, apply a standardised mineralogy to emitted

dust, and assume a constant proportion of bio-available iron in dust that is transported to oceans. This approach clearly exacerbates the uncertainties in radiative impact and, perhaps ultimately even more importantly, will compromise the realism of simulations to evaluate the role of dust in atmospheric chemistry and ocean fertilisation.

Testing and validation of dust-cycle models is hampered by the relative paucity of observations. Furthermore, the ability to simulate present-day conditions is not a sufficient test of model performance; the ability to reproduce the known and large changes in the dust cycle during e.g. glacial periods is crucial in order to build confidence in future predictions of changes in atmospheric dust loading and, hence, climate forcing. The DIRTMAP database was originally conceived as a tool for model validation under both modern and palaeo-conditions. The original version of this database (Kohfeld and Harrison, 2001) contained records from dust traps, from marine and ice cores, and from a limited number of terrestrial sites. Additional terrestrial sites were incorporated in an updated version presented in Kohfeld and Tegen (2007). However, neither version of the database reflects the considerable amount of recent work that has generated new records of dust deposition, better characterisation of the physical and biological properties of dust deposits, and improved chronological control on new and existing records.

These uncertainties and concerns have motivated the formation of a Working Group on Dust by the QUEST (Quantifying Uncertainty in the Earth System: <http://quest.bris.ac.uk>) programme of the UK Natural Environmental Research Council (NERC). The QUEST Working Group on Dust is an international group of experts in all aspects of the dust cycle, which met for the first time in November 2007 to develop a strategy for collaborative research aimed at improving understanding of the dust cycle under past, present and future climates. Here we summarise some of the key recommendations from this meeting.

Model improvements. Improved dust cycle modelling requires a major emphasis on the characterisation of dust source regions, building on the ongoing investigations of the geomorphic controls on dust emissions. Additionally, large improvements would result from improved description of the characteristics (particle size, mineralogy, shape) of deflated/airborne dust. New global data sets that allow the physical and chemical properties of material in potential source areas need to be developed, through refining global input data sets already available and using information derived from field studies. Continued work on the sensitivity of radiative forcing to the specification of dust physical properties is important as it will serve to guide the creation of such data sets.

Data requirements. Tools and protocols for benchmarking dust-cycle model simulations under modern and past conditions need to be developed. The DIRTMAP database provides a useful tool for validating spatial patterns in dust deposition under both present-day and palaeo-climates states, but urgently needs to be updated and expanded. The emphasis should be on including records from areas currently under-represented in the database, such as South America, Eurasia, the Middle East and the Southern Ocean. Priority should also be placed on the generation of high-resolution sediment records that document changes in dust deposition during climate oscillations, such as Dansgaard-Oeschger events. Documenting stratigraphic changes in size characteristics, and drawing on new high-resolution particle size analysis techniques that permit quantification of the sub-micron scale particles (highly relevant for modelling radiative effects) is

important. Mineralogical and isotopic information relevant to provenancing, radiative forcing and bio-fertilisation should be included in the database. Finally, because of the diversity of the records already included in the database, more metadata needs to be included to facilitate the selection of records for specific types of model evaluation in an objective way.

Modelling strategy. There are many opportunities for using observations and carefully-designed model simulations to understand changes in the dust cycle. Meso-scale models, for example, could provide an opportunity to test global model parameterisations of spatial heterogeneity in dust emissions. Dust-cycle feedbacks are not yet incorporated dynamically into simulations of past climates. There is clearly a need to design transient simulations with fully-coupled climate-dust models to address the potential role of dust in abrupt climate changes.

The next meeting of the QUEST Working Group on Dust, to be held in the autumn of 2008, will focus in more detail on dust-source modelling and characterisation. The QUEST Working Group on Dust is an inclusive group and invites participation from all scientists working on the dust cycle, though most particularly observationalists and modellers interested in aspects of the palaeo-dust cycle.

For more information, please visit: <http://www.bridge.bris.ac.uk/projects/dust>

References

- Balkanski, Y., M. Schulz, and T. Claquin, Reevaluation of Mineral aerosol radiative forcings suggests a better agreement with satellite and AERONET data, *Atmospheric Chemistry and Physics*, 7, 81-95, 2007.
- Forster, P., V. Ramaswamy, P. Artaxo, T. Berntsen, R. Betts, D.W. Fahey, J. Haywood, J. Lean, D.C. Lowe, G. Myhre, J. Nganga, R. Prinn, G. Raga, M. Schulz, and R.V. Dorland, Climate Change 2007: The Physical Science Basis. *Contribution of Working Group I to the Fourth Assessment Report of the Intergovernmental Panel on Climate Change*, edited by S. Solomon, D. Qin, M. Manning, Z. Chen, M. Marquis, K.B. Averyt, M. Tignor, and H.L. Miller, Cambridge University Press, Cambridge, United Kingdom and New York, NY, USA, 2007.
- Kohfeld, K., and I. Tegen, Record of Mineral Aerosol and their Role in the Earth System, in *Treatise on Geochemistry*, edited by K. Turekian, and H.D. Holland, pp. 1-26, Elsevier, 2007.
- Kohfeld, K.E., and S.P. Harrison, DIRTMAP: the geological record of dust, *Earth-Science Reviews*, 54 (1-3), 81-114, 2001.

Improved seawater thermodynamics:- How should the proposed change in salinity be implemented?

by SCOR/IAPSO Working Group 127

Membership of SCOR/IAPSO Working Group 127 on "Thermodynamics and the Equation of State of Seawater": Trevor J. McDougall, Chair, Chen-Tung Arthur Chen, Rainer Feistel, Valentina N. Gramm-Osipova, David R. Jackett, Brian A. King, Giles M. Marion, Frank J. Millero, Petra Spitzer, Dan Wright. Associate Member: Peter Tremaine, Corresponding author: Trevor.McDougall@csiro.au

Background

The SCOR/IAPSO Working Group 127 on the "Equation of State and Thermodynamics of Seawater" is charged with providing improved algorithms and descriptions of the thermodynamic properties of seawater. The working group has made significant progress on many of its goals, and it is now time to seek the advice of the oceanographic community regarding the best practical ways of adopting these developments into oceanographic practice. The Working Group has met twice to date, once in Warnemünde in 2006, then in Reggio Calabria in 2007. Our next meeting is in Berlin in September 2008.

The working group will soon provide the most accurate algorithms to date for the thermodynamic properties of seawater (such as density, entropy, enthalpy, specific heat capacity, etc). In order to achieve such accuracy it became evident that a salinity variable is required that more accurately represents absolute salinity than does the conductivity-based Practical Salinity. Spatial variations in the composition of seawater upsets the relationship between Practical Salinity S (which is a function of conductivity, temperature and pressure) and Absolute Salinity S_A (defined as the mass of dissolved material per mass of seawater solution). If the thermodynamic properties of seawater are to be written in terms of just one type of salinity, then they are much closer to being functions of (S_A, t, p) than being functions of (S, t, p) . Moreover, Absolute Salinity is a conservative property (that is, it is conserved when turbulent mixing occurs) whereas Practical Salinity is not conservative.

Absolute salinity for seawater of Reference Composition

In order to progress toward evaluating Absolute Salinity our first task was to define the relative concentrations of the constituents of Standard Seawater. This we have done, and this work is published in Millero et al (2008a). The abstract of this paper is as follows.

"Fundamental determinations of the physical properties of seawater have previously been made for Atlantic surface waters, referred to as "Standard Seawater". In this paper a Reference Composition consisting of the major components of Atlantic surface seawater is determined using these earlier analytical measurements. The stoichiometry of sea salt introduced here is thus based on the most accurate prior determination of the composition, adjusted to achieve charge balance and making use of the 2005 atomic weights. Reference Seawater is defined as any seawater that has the Reference Composition and a new Reference-Composition Salinity S_R is defined to provide the best available estimate of the Absolute Salinity of both Reference Seawater and the Standard Seawater that was used in the measurements of the physical properties. From a practical point of view, the value of S_R can be related to the Practical Salinity S by

$$S_R = (35.165\ 04 / 35) \text{ g kg}^{-1} \times S.$$

Reference Seawater that has been "normalized" to a Practical Salinity of 35 has a Reference-Composition Salinity of exactly $S_R = 35.165\ 04 \text{ g kg}^{-1}$.

The new independent salinity variable S_R is intended to be used as the concentration variable for future thermodynamic functions of seawater, as an SI-based extension of Practical

Salinity, as a reference for natural seawater composition anomalies, as the currently best estimate for Absolute Salinity of IAPSO Standard Seawater, and as a theoretical model for the electrolyte mixture "seawater".

As described in this abstract, for seawater of standard composition we have been able to relate the Absolute Salinity to the Practical Salinity; for example, at a Practical Salinity of 35, seawater of Reference Composition has an Absolute Salinity of $35.165\ 04 \text{ g kg}^{-1}$. We expect shortly to be able to recommend an algorithm that accounts for the variation of seawater composition from the standard composition. That is, we soon expect to be able to recommend an algorithm $S_A = S_A(S_R, \dots)$ where the extra arguments will be either measured parameters (such as total alkalinity, silicate and nitrate) or more simply the spatial locations longitude, latitude and pressure. Millero and Kremling (1976), Millero (2000) and Millero et al (2008b) are precursor papers to such an algorithm.

Advantages of Absolute Salinity over Practical Salinity

Absolute Salinity has the following advantages over Practical Salinity for oceanographic use.

1. The definition of Practical Salinity S on the PSS-78 scale is separate from the system of SI units. Absolute Salinity can be expressed in the unit (g kg^{-1}) . Adopting this SI unit for salinity would terminate the ongoing controversies in the oceanographic literature about the use of "psu" or "pss" and make research papers more readable to the outside scientific community and consistent with SI.
2. The freshwater mass fraction of seawater is not $(1 - 0.001 S)$. Rather, it is $(1 - 0.001 S_A / (\text{g kg}^{-1}))$, where S_A is the Absolute Salinity, defined as the mass fraction of dissolved material in seawater. The values of $S_A / (\text{g kg}^{-1})$ and S are known to differ by about 0.5%. There seems to be no good reason for continuing to ignore this known difference, e.g., in ocean models.
3. PSS-78 is limited to the salinity range 2 to 42. For a smooth crossover on one side to pure water, and on the other side to concentrated brines up to saturation, as e.g. encountered in sea ice at very low temperatures, salinities beyond these limits need to be defined. While this poses a challenge for S , it is not an issue for S_A .
4. The theoretical Debye-Hückel limiting laws of seawater behavior at low salinities, used for example in the determination of the Gibbs function of seawater, can only be computed from a chemical composition model, which is available for S_R but not for S .
5. For artificial seawater of Reference Composition, S_R has a fixed relation to Chlorinity, independent of conductivity, salinity, temperature, or pressure.
6. The next largest improvement in the equation of state of seawater will come from incorporating variations in the composition of seawater, that is, from calling the equation of state with Absolute Salinity rather than with Reference Salinity. The determination of Absolute Salinity is facilitated by the introduction of the Reference Composition and Reference Salinity.
7. Absolute Salinity S_A is a conservative variable, whereas, in the presence of compositional variations, Practical Salinity S (which is essentially determined by conductivity alone)

is not a conservative variable. All of our oceanographic practice assumes that “salinity” is a conservative variable (e.g. ocean model codes, the practice of mixing along straight lines on salinity-potential temperature diagrams, inverse modelling etc).

Expanding on point 7 above, it seems clear that we presently use Practical Salinity S as though it is a conservative variable, and yet we now know that it is not; for a given Absolute Salinity, Practical Salinity varies by up to 0.02 between different major ocean basins (Millero, 2000). This non-conservative regional variation in Practical Salinity is at least seven times the error with which salinity can be measured by modern instrumentation at sea. This difference of 0.02 in Practical Salinity causes differences in density that are also several times greater than the remaining uncertainty in the best algorithms for the density of seawater. It seems that in our oceanographic practice we intuitively ascribe the conservative properties of Absolute Salinity to our “salinity” variable, which to date has been Practical Salinity. For example, if we were intent on interpreting the salinity of an ocean model as Practical Salinity, then the salt conservation equation should contain a non-conservative source term to take account of the spatial variations in the composition of seawater.

Here we summarize the reasons why Absolute Salinity is the preferred salinity variable for oceanographic research.

- It will be preferred by journals since it is an SI unit.
- It is the natural salinity variable for ocean models since they assume that their salinity variable is conservative, hence it should be used to initialize ocean models at all depths.
- It is the natural variable to use in inverse models, budget studies and on salinity-temperature diagrams because its conservative nature justifies turbulent mixing occurring along straight lines on such a diagram.
- The freshwater fraction and the meridional freshwater flux follow naturally when using Absolute Salinity but not when using Practical Salinity.
- By using Absolute Salinity in the algorithm for the equation of state, the effects of the spatial variations of seawater composition are accounted for, while if Practical Salinity is used in such a call to the equation of state, a density error is incurred.
- It is the common salinity variable used in engineering, natural and geosciences outside oceanography, where Practical Salinity is often unknown or misconstrued.
- It is applicable to low concentrations in brackish lagoons and river mouths, to high concentrations in freezing or desiccating brines, as well as at higher temperatures in desalination plants, whereas Practical Salinity is defined only in the range $2 < S < 42$.
- If necessary for chemical or biological reasons, all partial ion concentrations in a sample are easily available, to which Practical Salinity is unrelated.

The SCOR/IAPSO Working Group 127 regards these as compelling reasons for adopting Absolute Salinity as the new preferred salinity variable in the analysis of oceanographic data. Accordingly we are formulating new algorithms for density, enthalpy, entropy, potential temperature, sound speed, etc in terms of Absolute Salinity, temperature and pressure (Feistel (2008)). The extended validity range of the new formulas in temperature and salinity precludes using Practical Salinity as the independent variable of these thermodynamic quantities. For example, *in situ* density will have the functional form and potential temperature will have the functional form $\theta(S_A, t, p, p_r)$ Absolute Salinity S_A will be defined as $S_A = S_R + \delta S_A$ where Reference salinity S_R is simply proportional to Practical

Salinity S as described in Millero et al (2008), namely by

$$S_R = (35.16504 / 35) \text{ g kg}^{-1} \times S,$$

and δS_A is the difference between Absolute and Reference Salinities. δS_A will be available as a look up table as a function of latitude, longitude and pressure and also as an alternative linear relationship of nutrient and silicate concentrations, or for example, as a Calcium excess estimate from the river discharge into estuaries. We expect to have algorithms available before the end of 2008.

How to adopt Absolute Salinity?

Having made the case that Absolute Salinity possesses many advantages over Practical Salinity, how should present oceanographic practice adapt to incorporate these advantages?

The obvious thing to do would be to decide on a date on which the whole community ceases to use Practical Salinity and switches to using Absolute Salinity. However the algorithm to convert Reference Salinity to Absolute Salinity is less mature and will probably remain a “work in progress” for several years. Moreover, data that are stored in archives should have a very close connection to a measurement (like temperature or conductivity) rather than being the result of an algorithm that is likely to change with time. Hence one cannot really imagine storing Absolute Salinity in data bases. Rather, the closest thing to do in this vein is to store Reference Salinity.

Storing Reference Salinity in data centres would have the advantage that it is an SI unit. However before the equation of state (or other thermodynamic quantities) can be evaluated using the new software, the Reference Salinity data need to be converted to Absolute Salinity using the most up-to-date version of this software. Moreover, the community cannot completely abandon Practical Salinity since it will remain as the salinity variable in the archives for cruises undertaken before the change-over date. By changing the salinity variable that is reported from cruises to data bases from Practical Salinity to Reference Salinity the possibility of contamination of the data archives arises as salinity of one type is incorrectly labeled and stored as the other type of salinity.

In the long run, as with many other historical non-SI units like torr, cal or dyn, it would seem to be an advantage to use only Reference Salinity and abandon the use of Practical Salinity completely. If Reference Salinity were the salinity variable to be used in all of the revised thermodynamic algorithms, the argument for “biting the bullet” and abandoning Practical Salinity as much as possible would seem to be the correct path. But it is Absolute Salinity that we seek, and Reference Salinity is only part way towards the evaluation of Absolute Salinity. Given this, is it worthwhile changing the present archiving practice in favour of a variable (Reference Salinity) that is still not the final salinity that we will use (Absolute Salinity)?

Any choice of action inherently involves compromises, and the best course of action is not obvious to the Working Group. As a way of focusing the discussion we outline two possible routes for adopting the advantages of Absolute Salinity, labeled Option 1 and Option 2.

Option 1

- Change from reporting Practical Salinity to reporting Reference Salinity to national and international data bases. This implies that the data bases store Practical Salinity from the old cruises and store Reference Salinity from new cruises (from say 1st January 2010).
- Provide software (for example, of the form $S_A(S_R, x, y, p)$) to produce the best available estimate of Absolute Salinity from Reference Salinity (using additional information on

position or water properties).

- Have all the thermodynamic software in the form $p(S_A, t, p)$.

Discussion of Option 1

The main advantage of Option 1 is that the community eventually ceases to use the non-SI unit Practical Salinity, and instead uses the two SI salinity measures, Reference Salinity and Absolute Salinity.

A drawback of Option 1 is that there will be cases of contamination of the data bases where cruise salinity is labeled and stored as Reference Salinity whereas in fact it is Practical Salinity data, and vice versa. This kind of error presently contaminates the temperature, oxygen and pressure/depth data bases.

Since both S and S_R are simply measures of conductivity, and since they are simply proportional to each other, will it be seen that we are taking a course of action that has potential for confusion for only academic benefit?

Recall that scientific work and papers are mostly done with potential temperature θ rather than in situ temperature t so the first thing that one usually does with the S, t, p data from a data centre is to form θ . Similarly, scientific work and papers should be done with Absolute Salinity rather than Reference Salinity so the first thing that one needs to do under Option 1 with the S_R, t, p data from a cruise or from a data centre is to form not only θ but also S_A . This analogy with what we already do with storing the measured variable t but using the derived variable θ is very close.

Under Option 1 we cannot imagine that the community can altogether forget about Practical Salinity however, as the data from older cruises (e.g. all of WOCE) is stored in data centres in terms of Practical Salinity. This data will need converting first to Reference Salinity and then to Absolute Salinity before the thermodynamic routines such as potential temperature, density, potential enthalpy etc, can be called by oceanographic researchers.

There will be some instances when the new software is called with the salinity data being S and in those instances an error will be made. This type of error is an undesirable consequence of both Options 1 and 2.

Option 1 requires manufacturers (such as Seabird) to change what they presently do. The instruments will need to output their salinity in terms of Reference Salinity. Also the ampoules of standard seawater will need to quote their salinity in terms of Reference Salinity. The transition date of say 1st January 2010 has to be handled very carefully in these respects. Further, anyone wanting to make use of older ampoules will have to be aware of the transition and how to deal with it.

Option 2

- Continue to report Practical Salinity S from cruises and to have only Practical Salinity S stored at national and international data centres.
- Provide software (for example, of the form $S_A(S, x, y, p)$) to produce the best available estimate of Absolute Salinity from Practical Salinity (using additional information on position or water properties).
- Have all the thermodynamic software in the form $p(S_A, t, p)$.

Discussion of Option 2

By reporting only S in data bases we would expect to greatly reduce the possibility of salinity data being mislabeled in data bases.

Since both S and S_R are simply measures of conductivity, option 2 is consistent with the argument that there is little value

in replacing one measure of conductivity (namely Practical Salinity) with another (namely Reference Salinity) in data bases. Rather, under Option 2 data centres store S and S alone.

As mentioned above, scientific work and papers are mostly done with potential temperature θ rather than *in situ* temperature t so the first thing that one usually does with the S, t, p data from a data centre is to form θ . Similarly, scientific work and papers will be mostly done with Absolute Salinity rather than Practical Salinity so the first thing that one needs to do under Option 2 with the S, t, p data from a cruise or from a data centre is to form not only θ but also S_A . This analogy with what we already do with storing the measured variable t but using the derived variable θ suggests that storing S but using S_A will not cause oceanographers any serious difficulties.

There will be some instances when the new software is called with the salinity data being S and in those instances an error will be made. This type of error is an undesirable consequence of both Options 1 and 2. However this error will affect the results and the publications arising out of those who make this error, but this error will not contaminate an archived data set.

Option 2 does not require manufacturers (such as Seabird and the Standard Seawater Service) to change what they presently do. Rather, Option 2 puts the responsibility for the changes in the hands of practicing research oceanographers.

Request for your input

The above two options are just two of many options; please do not feel constrained in your comments to these options. We seek input from the oceanographic community on how to gain the advantages of adopting Absolute Salinity in our oceanographic research work. The key issue seems to revolve around which type of salinity is required to be reported to and archived by oceanographic data centres. We encourage frank responses. Each response will be thoughtfully considered by the Working Group.

Please email your comments to trevor.mcdougall@csiro.au with the words "Comment for WG127 on how to adopt Absolute Salinity" as the message title.

References

- Feistel, R., 2008: A Gibbs Function for Seawater Thermodynamics for $-6\text{ }^{\circ}\text{C}$ to $80\text{ }^{\circ}\text{C}$ and Salinity up to 120 g kg^{-1} . submitted to *Deep-Sea Research I*, November 2007.
- Millero, F. J., 2000: Effect of changes in the composition of seawater on the density-salinity relationship. *Deep-Sea Research*, **47**, 1583-1590.
- Millero, F. J., R. Feistel, D. G. Wright and T. J. McDougall, 2008a: The composition of Standard Seawater and the definition of the Reference-Composition Salinity Scale. *Deep-Sea Research I*, **55**, 50-72.
- Millero, F. J. and K. Kremling, 1976: The densities of Baltic Sea Waters. *Deep-Sea Research*, **23**, 1129-1138.
- Millero, F. J., J. Waters, R. Woosley, F. Huang and M. Chanson, 2008b: The effect of composition on the density of Indian Ocean waters. *Deep-Sea Research I*, in press.

PACSWIN: A new international ocean climate program in the Indonesian seas and adjacent regions

You, Y.^{1,*}, T. Rossby², W. Zenk³, A. Gordon⁴, A.G. Ilahude⁵, N. Sugino⁶, R. Davis⁷, D. Hu⁸, D. Susanto⁴, P.L. Richardson⁹, C. Villanoy¹⁰, C.-T. Liu¹¹, K. Kim¹², R. Molcard¹³, M. Fukasawa⁶, W.W. Pandoe¹⁴, D.J. Baker¹⁵, M. Koga¹⁶, T. Qu¹⁷, R. Fine¹⁸, A. Gabric¹⁹, R. Robertson²⁰, Y. Masumoto²¹, S. Riser²²

¹University of Sydney Institute of Marine Science (USIMS), Australia, ²Graduate School of Oceanography, University of Rhode Island, USA., ³IFM-GEOMAR, Leibniz-Institut für Meereswissenschaften, ⁴Department of Earth and Environmental Sciences, Lamont-Doherty Earth Observatory (LDEO), USA., ⁵Department of Marine and Fisheries (BPPT) and Jl. Indonesia., ⁶Institute of Observational Research for Global Change, JAMSTEC, Japan., ⁷Scripps Institute of Oceanography (SIO), USA., ⁸Lab. of Ocean Circulation and Wave Studies, Institute of Oceanology, Chinese Academy of Sciences, China, ⁹Woods Hole Oceanographic Institution (WHOI), USA., ¹⁰Marine Science Institute, University of the Philippines, Philippines, ¹¹Institute of Oceanography, National Taiwan University, Taiwan, ¹²School of Earth and Environmental Sciences (SEES), Seoul National University, Korea, ¹³LOCEAN – IPSL, Université Pierre et Marie Curie, France, ¹⁴Technology Center for Marine Survey – BPPT, Indonesia, ¹⁵8031 Seminole Avenue, Philadelphia, USA., ¹⁶Physical Oceanogr. Lab., Univ. of the Ryukyus, Japan, ¹⁷International Pacific Research Center, School of Ocean and Earth Science and Technology, University of Hawaii, USA., ¹⁸RSMAS/MAC, University of Miami, USA., ¹⁹Griffith School of the Environment, Griffith University, Australia, ²⁰School of Physical, Environmental and Mathematical Sciences, Australian Defence Force Academy, Australia, ²¹Dept. of Earth and Planetary Science, Graduate School of Science, Univ. of Tokyo, Japan, ²²School of Oceanography, University of Washington, USA.

Corresponding author: you@geosci.usyd.edu.au

1. Introduction

The UN Climate Change Conference - recently held in Bali, Indonesia - has set up a road map to replace the Kyoto Protocol by 2012. Strong messages from the conference were the high level of governmental awareness of global warming and its consequences, the critical need for effectively monitoring climate change, and provision of accurate information to society. But adequate ocean monitoring for climate change is still lacking, and will hinder our ability to forecast and provide that accurate information. Nowhere is this more evident than in the critical Indonesian Throughflow region between the Pacific and Indian Oceans.

Following the end in 2006 of the International Nusantara Stratification and Transport (INSTANT) program there is no longer any ocean climate monitoring program existing in the Indonesian seas and adjacent regions. Moreover, the present Argo program does not cover the Indonesian seas. A different monitoring strategy, therefore, needs to be implemented so that Indo-Pacific ocean climate variability and change can be properly monitored. Here we propose a new international coordinated ocean climate program: Indonesian ThroughFlow: PACific Source Water Investigation (ITF:PACSWIN; hereafter we simply call PACSWIN) dedicated for that purpose.

Interest in the climate impact of global warming on the weakening or even halting of the meridional overturning circulation (MOC) in the northern North Atlantic has largely overshadowed the ITF as an important component of global circulation and climate change. New observational programs to monitor the MOC in the North Atlantic have been carried out recently and preliminary results show remarkable variability of the currents (Church, 2007; Kanzow et al., 2007; Cunningham et al., 2007) which must be incorporated into any predictive models.

PACSWIN (see yellow dashed line in Figure 1, page 18 and its logo in the top left corner of the figure) will be carried out in the Indonesian seas and adjacent regions. In particular, PACSWIN focuses on the entrance for Pacific source waters including those east of Mindanao, northern Papua New Guinea (PNG) water and the far western equatorial Pacific and the exit of the ITF to the eastern Indian Ocean, as well as possible reverse flow from the Indian Ocean. The task is to better identify various Pacific and Indian Ocean source waters and the Indo-Pacific water mass exchange via the ITF linkage with current systems east of Mindanao and north of PNG, the equatorial current system and the currents of the eastern Indian Ocean, which INSTANT could not resolve.

The PACSWIN approach will include extended tracers including temperature, salinity, nutrients and biological and chemical tracers. We want to address how various Pacific source waters are transformed to become new members for the Indian Ocean and how various waters are transformed by tidal and vertical mixing processes within the Indonesian seas.

2. The water-mass structure in the Indonesian seas

It is reasonable to expect that the potential dramatic climate

change associated with weakening of ocean circulation in the northern North Atlantic could affect the ITF and cause consequent regional climate change in the southeast Asia and Australia because the ITF is a choke point of the global ocean circulation affecting the earth's climate. Ocean climate change seems to be happening now not only in the North Atlantic but also in the Indo-Pacific region. It is clear that learning more about the ITF will have potential regional and world-wide benefits.

The Indonesian seas link the warm pools of the western Pacific and eastern Indian Ocean. The former regulates the global heat budget and so provides controls on the atmospheric circulation. The latter guides the Indian monsoon circulation and African drought through the Indian dipole mode [Saji et al., 1999]. The Indonesian archipelago is geographically complicated including many shallow and deep straits and interior basins. The Sulawesi Sea (or Celebes Sea) and Banda Sea are among the largest and deepest of the region. The unique geographic condition and strong tides enable the blending of incoming Pacific source waters into a different water mass. The primary source of the ITF is from the North Pacific thermocline and intermediate water carried by the Mindanao Current into the Sulawesi Sea, through the Makassar Strait into the Flores Sea and Banda Sea and finally to the eastern Indian Ocean via either side of Timor with a small amount flowing out from Lombok Strait (Wyrtki, 1961; Gordon, 1986; Gordon and Fine, 1996).

An additional ITF pathway in the lower thermocline, intermediate and deep water, of South Pacific origin, is derived through the eastern route, via the Maluku (or Molucca) and Halmahera Seas into the Banda Sea (Cresswell and Luick, 2001). Since the Timor and Banda Seas are on the western side connecting the eastern Indian Ocean with a sill depth of over 1500 m, the influence of Indian water seems inevitable, especially during La Nina (Molcard et al., 1996). The Indian Ocean reverse flow is also observed in data from recent moorings (Gordon et al., 2006).

The thermohaline [T-S] stratification and water mass structure of the Indonesian seas (see Figure 2, page 18 and Table 1) can be summarized as upper thermocline water with a salinity maximum at 130 m (or $24.5\sigma_\theta$) (South Pacific Subtropical Water (SPSW)), main thermocline water with relative high salinity and oxygen but no extrema at 220 m (North Pacific Subtropical Water (NPSW)), a salinity minimum at 300 m (or $26.5\sigma_\theta$) (North Pacific Intermediate Water (NPIW)) (You, 2003), a relative low salinity and oxygen but no extrema at 1000 m (or $27.25\sigma_\theta$) (Antarctic Intermediate Water (AAIW)) and deep water with a relative high salinity below 1500 m (or larger than $27.4\sigma_\theta$) (Ilahude and Gordon, 1996; Field and Gordon, 1992; Hautala et al., 1996). Note that the sill depth in the Maluku Sea and Lifamatola Strait is sufficiently deep to allow upper Circumpolar Deep Water (uCDW) from the Southern Ocean to get into the Banda Sea.

But the pathways of the remote Pacific sources into the Indonesian seas have not been well resolved. Spatially, the

water-mass structure in the western route is better resolved than the eastern route, because the western route is predominated by North Pacific sources and is shallower with sill control of about 600 m (implying less water types involved). The eastern route is mixed by both North and South Pacific sources. A teleconnection of the Indonesian water types with the remote Pacific source waters has to be established in extended property fields including nutrients and chemical tracers. For example, it is still unclear whether or not there is a shortcut by North Pacific source waters from the Mindanao Current (MC) southward along east of Sangihe Ridge to the Maluku Sea, and a circulation path by South Pacific source water to the MC through the equatorial current system (Godfrey, 1996), and how much South Pacific source water successfully crosses the Lifamatola Passage although evidence is building up that water of South Pacific origin does get into the Halmahera and Maluku Seas (Cresswell and Luick, 2001; Talley and Sprintall, 2005). The model results of Zenk et al. (2005) show that South Pacific waters not only feed the Halmahera Sea and Maluku Sea but probably also the southern Sulawesi Sea though with a strong seasonal dependence.

3. Future perspective

A successful PACSWIN will require a truly strong international effort. The survey plans, instruments and technologies need to be well coordinated among many participating countries and international organizations, especially those in the Asia-Pacific region. A time span of about two years for pilot studies and three years for operation is currently suggested. Some long-term monitoring projects such as submarine cables will be needed for as long as possible.

PACSWIN has set three priority monitoring projects: submarine cables, floats and moorings. An international submarine cable workshop on cable voltage measurement to monitor transport through straits is planned to be held in Pusan, Korea April 2009. PACSWIN will integrate with other two proposed ocean programs, SPICE (Southwest Pacific Ocean Circulation and Climate Experiment) and NPOCE (Northwestern Pacific Ocean Circulation Experiment) to constitute a major ocean climate monitoring network in the Indo and western Pacific for at least the coming decade.

Sponsorship will be sought for the PACSWIN program from individual participating national governments and funding agencies including governmental sectors and the private sector. The endorsement of international organisations such as WCRP (CLIVAR), IOC, SCOR and APEC will also be sought. Support from the Indonesian scientific community and government and collaboration with international community will be required to assure the success of this international program.

Acknowledgments

This article is dedicated in memory of Prof. Nobuo Sugimoto, who passed away on January 29, 2007. Dr. George Cresswell made useful comments on an earlier version of the manuscript.

References

Church, J. A., A change in circulation? *Science*, **37**, 908-909, 2007.

Cresswell, G. R. and J. L. Luick, Current measurements in the Halmahera Sea, *J. Geophys. Res.*, **106**, 13945-13952, 2001.

Cunningham, S. A., T. Kanzow, D. Rayner, M. O. Baringer, W. E. Johns, J. Marotzke, H. R. Longworth, E. M. E. M. Grant, J. J.-M. Hirschi, L. M. Beal, C. S. Meinen and H. L. Bryden, Temporal variability of the Atlantic meridional overturning circulation at 26.5°N, *Science*, **37**, 935-938, 2007.

Ffield, A. and A. L. Gordon, Vertical mixing in the Indonesian thermocline, *J. Phys. Oceanogr.*, **22**, 184-195, 1992.

Godfrey, J. S., The effect of the Indonesian Throughflow on ocean circulation and heat exchange with the atmosphere: A review. *J. Geophys. Res.*, **101**, 12217-12238, 1996.

Gordon, A. L., Inter-ocean exchange of thermocline water. *J. Geophys. Res.*, **91**, 5037-5046, 1986.

Gordon, A. L. and R. A. Fine, Pathways of water between the Pacific and Indian Oceans in the Indonesian seas, *Nature*, **379**, 146-149, 1996.

Gordon, A. L., I. Soesilo, I. Brodjonegoro, A. Ffield, I. Jaya, R. Molcard, J. Sprintall, R. D. Susanto, H. van Aken, S. Wijffels and S. Wirasantosa, The first 1.5 years of INSTANT data reveal the complexities of the Indonesian Throughflow, *CLIVAR Exch.*, **11**, 10-11, 2006.

Hautala, S. L., J. L. Reid and N. Bray, The distribution and mixing of Pacific water masses in the Indonesian seas, *J. Geophys. Res.*, **101**, 12375-12389, 1996.

Ilahude, A. G. and A. L. Gordon, Thermocline stratification within the Indonesian seas, *J. Geophys. Res.*, **101**, 12401-12409, 1996.

Kanzow, T., S. A. Cunningham, D. Rayner, J. J.-M. Hirschi, W. E. Johns, M. O. Baringer, H. L. Bryden, L. M. Beal, C. S. Meinen and J. Marotzke, Observed flow compensation associated with the MOC at 26.5°N in the Atlantic, *Science*, **37**, 938-941, 2007.

Molcard, R., M. Fieux and A. G. Ilahude, The Indo-Pacific throughflow in the Timor Passage, *J. Geophys. Res.*, **101**, 12411-12420, 1996.

Saji, N. H., B. N. Goswami, P. N. Vinayachandran and T. Yamagata, A dipole mode in the tropical Indian Ocean, *Nature*, **401**, 360-363, 1999.

Talley, L. D. and J. Sprintall, Deep expression of the Indonesian throughflow: Indonesian Intermediate Water in the South Equatorial Current, *J. Geophys. Res.*, **110**, doi:10.1029/2004JC002826, 2005.

Wyrki, K., Scientific results of marine investigations of the South China Sea and the Gulf of Thailand, 1959-1961, volume 2, Physical oceanography of southeast Asian waters, *NAGA Rep. 2*, Scripps Inst. of Oceanogr., Univ. of Calif., San Diego, La Jolla, 195 pp. 1961.

You, Y. and M. Tomczak, Thermocline circulation and ventilation in the Indian Ocean derived from water mass analysis, *Deep-Sea Res. I*, **40**, 13-56, 1993.

You, Y., The pathway and circulation of North Pacific Intermediate Water, *Geophys. Res. Lett.*, **30** (24), doi:10.1029/2003GL018561, 2003.

Zenk, W., G. Siedler, A. Ishida, J. Holfort, Y. Kashino, Y. Kuroda, T. Miyama and T. Müller, Pathways and variability of the Antarctic Intermediate Water in the western equatorial Pacific Ocean, *Prog. Oceanogr.*, **67**, 245-281, 2005.

Water mass name in the Indonesian seas	Source characteristics	Origin of Pacific	Contributing to new source of the Indian Ocean
NPSW	high S, T and O ₂ low nutrients path: via Makasar Strait	shallow subtropical North Pacific	AAMW low S, T high silicate
SPSW	high S, T, O ₂ low nutrients path: via Halmahera Sea	shallow subtropical South Pacific	AAMW low S, T high silicate
NPIW	S minimum path: via Makasar and Maluku Sea	Okhotsk Sea and Gulf of Alaska	AAMW low S, T high silicate
AAIW	S minimum, high O ₂ low nutrients path: via Maluku Sea, Seram Sea, Banda Sea to Timor Sea	southeast South Pacific	IIW silicate maximum
uCDW	high S and nutrients low T and O ₂ path: via Maluku Sea, Seram Sea to Banda Sea	circumpolar region of the Southern Ocean	none

Table 1. Inventory of water masses in the Indonesian seas and their teleconnection with the Pacific source formation and transformation to new source of the Indian Ocean.

Contents

Obituary	1
Editorial	1
A View from the Golden Years of the North American Monsoon Experiment	1
Atmospheric simulations of the 2004 North American Monsoon circulation: NAMAP2	6
Relationships between Gulf of California moisture surges and tropical cyclones in the eastern Pacific Basin	9
Relationship of TEWs and spatial-temporal variability of MCSs in the North American Monsoon Region	9
Radar-based studies of convection in NAME	12
GPS observations of precipitable water and implications for the predictability of precipitation during the North American Monsoon	14
Relation between surface flux measurements and hydrologic conditions in a subtropical scrubland during the North American Monsoon	21
Extended west-wide seasonal hydrological system: Seasonal hydrological prediction in the NAMS region	24
The QUEST Working Group on Dust and the future of dust-cycle research	25
Improved seawater thermodynamics: - How should the proposed change in salinity be implemented?	27
PACSWIN: A new international ocean climate program in the Indonesian seas and adjacent regions	30

The CLIVAR Newsletter Exchanges is published by the International CLIVAR Project Office
ISSN No: 1026 - 0471

Editors: Dave Gochis and Howard Cattle
Layout: Sandy Grapes
Printing: Technart Limited, Southampton, United Kingdom

CLIVAR Exchanges is distributed free of charge upon request (email: icpo@noc.soton.ac.uk)

Note on Copyright

Permission to use any scientific material (text as well as figures) published in CLIVAR Exchanges should be obtained from the authors. The reference should appear as follows: Authors, Year, Title. CLIVAR Exchanges, No. pp. (Unpublished manuscript).

The ICPO is supported by the UK Natural Environment Research Council and NASA, NOAA and NSF through US CLIVAR.

If undelivered please return to:
International CLIVAR Project Office
National Oceanography Centre Southampton
University of Southampton Waterfront Campus
Southampton, SO14 3ZH, United Kingdom
<http://www.clivar.org>



Please recycle this newsletter by passing on to a colleague or library or disposing in a recognised recycle point